MINK1 modulates 5FU resistance in OSCC through AKT/MDM2 mediated regulation of p53.

One sentence summary: Lestaurtinib reverses 5FU sensitivity in drug resistant OSCC.

Sibasish Mohanty[#1,2], Pallavi Mohapatra[#1,2], Omprakash Shriwas[1], Manashi Priyadarshini[1,3], Shamima Azma Ansari[1,2], Swatismita Priyadarsini[1], Rachna Rath[4], Mahesh Sultania[5], Saroj Kumar Das Majumdar[6], Rupesh Dash[1*]

1. Institute of Life Sciences, Bhubaneswar, Odisha, India-751023

2. Regional Center for Biotechnology, Faridabad, India.

3. KIIT School of Biotechnology, KIIT University, Bhubaneswar, India.

4. Dept. of Oral & Maxillofacial Pathology, SCB Dental College & Hospital, Cuttack, Odisha, India- 753007

5. Department of Surgical Oncology, All India Institute of Medical Sciences, Bhubaneswar, Odisha, India-751019

6. Department of Radiotherapy, All India Institute of Medical Sciences, Bhubaneswar, Odisha, India-751019

[#] Authors contributed equally

[*] Corresponding authors

Rupesh Dash, Institute of Life Sciences, Nalco Square, Chandrasekharpur, Bhubaneswar-751023, Odisha, India. Phone: +91-674-2301460, Fax: +91-674-2300728, E-mail: rupesh.dash@gmail.com , rupeshdash@ils.res.in

Keywords:

MINK1, 5Fluorouracil, AKT, MDM2, p53, lestaurtinib, patient derived cells.

Abstract:

Cisplatin, 5FU and docetaxel (TPF) are the most common chemotherapy regimen used for advanced OSCC. However, many cancer patients experience relapse, continued tumor growth, and spread due to drug resistance, which leads to treatment failure and metastatic disease. Here, using a CRISPR/Cas9 based kinome knockout screening, Misshapen-like kinase 1 (MINK1) is identified as an important mediator of 5FU resistance in OSCC. Analysis of clinical samples demonstrated significantly higher MINK1 expression in the tumor tissues of chemotherapy non-responder as compared to chemotherapy responders. The in-vitro and xenograft experiments indicate that knocking out MINK1 restores 5FU mediated cell death in chemoresistant OSCC. An antibody based phosphorylation array screen revealed MINK1 as a negative regulator of p53. Mechanistically, MINK1 modulates AKT phosphorylation at Ser473, which enables p-MDM2 (Ser 166) mediated degradation of p53. We also identified lestaurtinib as a potent inhibitor of MINK1 kinase activity. Lestaurtinib significantly induces 5FU mediated cell death in chemoresistant OSCC lines. The patient derived chemoresistant cell based xenograft data suggest that lestaurtinib restores 5FU sensitivity and facilitates a significant reduction of tumor burden. Overall, our study suggests that MINK1 is a major driver of 5FU resistance in OSCC. The novel combination of MINK1 inhibitor lestaurtinib and 5FU needs further clinical investigation in advanced OSCC.

Introduction

Majority of head and neck cancer is originated from mucosal epithelium collectively termed as Oral squamous cell carcinomas (OSCC) (*1*). It is the most prevalent neoplasm in developing country like India with approximately 80000 new cases diagnosed every year (*2*). Unfortunately, most of the patients present with advanced OSCC are without having any preclinical history of pre malignant lesions. The treatment modalities for advanced OSCC includes surgical removal of tumor followed by concomitant chemoradiotherapy. Neoadjuvant chemotherapy is frequently prescribed for surgically unresectable OSCC tumors (*3*). However, despite of having all these treatment modalities the 5-year survival rate of advanced tongue OSCC is less than 50%. Chemoresistance is one of the major causes of treatment failure in OSCC(*4*). The chemotherapeutic regimen used for OSCC are cisplatin, 5FU and Docetaxel (TPF)(*3*). Though chemotherapy drugs show initial positive response, tumor acquires resistance gradually and patients experience continued tumor growth and metastatic disease.

Reprogramming resistant cells to undergo drug induced cell death is a viable way to overcome drug resistance. This can be achieved by identifying the causative factors for acquired chemoresistance and discovering novel agents to target critical causative factors, which will restore drug-induced cell death in chemoresistant OSCC. Kinases, which transfer a reversible phosphate group to proteins, play important role in regulating several phenotypes of carcinogenesis including growth, proliferation, angiogenesis, metastasis and evasion of antitumor immune responses (*5*). There are approximately 538 known kinases in human which are known to regulate different kinase signaling. A few of them are also known to regulate drug resistance in HNSCC. A kinome study revealed, microtubule-associated serine/threonine kinase 1 (MAST1) is a major driver of cisplatin resistance in HNSCC. MAST1 inhibitor lestaurtinib efficiently sensitized chemoresistant

cells to cisplatin. Overall, the study suggests that MAST1 is a viable target to overcome cisplatin resistance (*6*). Ectopic overexpression of receptor tyrosine kinase in HNSCC mediates acquired resistance against cetuximab. For example, hyper activation of AXL was observed in clinical samples those are resistant to cetuximab (*7*). It was also found that RAS-MAPK are key mediator for cetuximab resistance in OSCC (*8*). However, very limited studies are available about the kinases those mediate 5FU resistance in OSCC.

MINK1 belongs to germinal center kinase (GCK) family and it is involved in regulation of several important signaling cascades (*9*). Recently, it is reported that MINK1 can regulate the planner cell polarity, which is essential for spreading of cancer cells. The PRICKLE1 encodes the planner cell polarity protein that binds to MINK1 and RICTOR (a member in mTOR2 complex) and this complex regulates the AKT meditated cell migration. Selectively targeting either of MINK1, PRICKLE1 or RICTOR can significantly decrease the migration of cancer cell in breast carcinomas (*10*). Ste20-related kinase, misshapen (msn), a Drosophila homolog of MINK1 regulates embryonic dorsal closure through activation of c-jun amino-terminal kinase (JNK) (*11*).

The goal of this study is to find out the potential kinase(s) those are major driver(s) of 5FU resistance in OSCC, for which a CRISPR based kinome screening was employed on 5FU resistant OSCC lines. The top ranked protein MINK1 was selected for validation in multiple cell lines and patient derived cells. In addition to this, lestaurtinib was identified to inhibit MINK1 kinase activity, which can reverse 5FU mediated cell death in chemoresistant OSCC lines. Ultimately, we demonstrated that MINK1 regulates the p53 in 5FU resistant OSCC. MINK1 activates AKT by phosphorylation at Ser473, which phosphorylates MDM2 at Ser166, the later in turn triggers degradation of p53.

Results:

Establishment and characterization of 5FU resistant OSCC lines. The 5FU resistant OSCC lines were established by prolonged treatment of 5FU to OSCC cell lines as described in materials and methods. Monitoring the cell viability of 5FU sensitive (5FUS) and resistant (5FUR) pattern of H357, SCC4 and SCC9 cell lines by MTT assay suggest that 5FUR cells achieved acquired resistance (Fig. S1A,B). Enhanced cancer like stem cells (CSCs) and elevated expression of ATP-binding cassette (ABC) transporters are the hallmarks of chemoresistant cells. qRT-PCR data suggest that CSC markers (SOX2, OCT4 and NANOG) as well as majority of ABC transporters expression were elevated in 5FUR cells as compared to 5FUS cells (Fig. S1C, D).

Kinome wide screening identifies MINK1 as a potential driver of 5FU resistance in OSCC: To identify the kinases those play important role in 5FU resistance, a CRISPR based kinome-wide screening was performed using a lentiviral sgRNA library knocking out 840 kinases individually with a total number of 3214 sgRNA constructs. To target the individual kinase, upto 4 sgRNA lentiviral constructs were pooled together. For kinome screening, Cas9 overexpressing 5FU resistant OSCC lines were established (Fig. S2), which showed similar drug resistant pattern with parental 5FUR OSCC lines(Fig. S3A). We also determined the polybrene and puromycin tolerance concentration in Cas9 overexpressing clones (Fig. S3B, C). The 5FUS and 5FUR lines were treated with 5FU and cell death was measured in high content analyzer using a fluorescent cell viability

dye, the data suggest significantly lower cell death in 5FUR cells as compared to 5FUS cells, which is in harmony with the previously measured 5FU tolerance in both lines (Fig. S4A-C). The screening protocol was optimized using appropriate positive and negative control. When 6TG (6-Thioguanine) was treated to HPRT1 (Hypoxanthine Phosphoribosyltransferase 1) KO lines, which is used as positive control for screening, it showed resistance to cell death, whereas HPRT1 WT cells were sensitive to 6TG, suggesting optimized screening protocol (Fig. S4D, E). As a negative control, lentivirus expressing scrambled sgRNA was used.

For primary screening, the 5FU resistant line (H357 5FUR) was transduced with a lentivirus containing sgRNAs targeting each of the 840 individual kinases, after which sub lethal dose of 5FU was treated for 48h followed by measuring cell death in high content analyzer using a fluorescent cell viability dye (Fig. 1A). From primary screening, 334 kinases out of 840 were selected for further consideration by rejecting rest of sgRNA clones which alone induced cell death more than 30 % (Fig. 1B, C). The 60 candidate kinases having lowest survival fraction score were evaluated in the secondary screening using three more chemoresistant lines i.e SCC4 5FUR, SCC9 5FUR and H357 CisR. From the primary and secondary screening, MINK1, SBK1 and FKBP1A emerged as the only three common kinases among the 5FUR lines with MINK1 having the lowest survival fraction score, which sensitize the chemoresistant cell to 5FU mediated cell death the most (Fig. 1 C-E). In secondary screening, MINK1 knock out showed minimal efficacy in sensitizing cisplatin resistant cell lines to cisplatin (Fig. S5), indicating the specific role of MINK1 towards acquired 5FU resistance. Next, monitoring the expression of MINK1 in OSCC resistant lines, we found the expression of MINK1 is significantly higher in 5FUR lines as compared to 5FUS lines of OSCC (Fig. 1F). With the evaluation of clinical samples, the expression of MINK1 was found to be elevated in tumor tissues of chemotherapy non-responders as compared to chemotherapy responders (Fig. G, H). We also evaluated the MINK1 expression in drug-naive and post-CT nonresponder paired tumor samples from the same patient and observed that the post–CT-treated tumor samples showed higher MINK1 expression (Fig. I, J).

MINK1 is an important target to overcome 5FU resistance in OSCC: To confirm the finding from the kinome screening, MINK1KO (knock out) clones were generated, using lentivirus expressing two different sgRNAs, in Cas9 overexpressing 5FUR OSCC lines and patient derived line 2 (PDC2) (Fig. 2A). PDC2 was isolated and characterized earlier from tumor of chemotherapy-non-responder patient, who was treated with neoadjuvant TPF without any response (*12*). The colony forming and MTT assay data suggest that knocking out MINK1 significantly reduced the cell viability when the chemoresistant cells were treated with 5FU (Fig. 2B, C). Here onwards we used sgRNA 1 for rest of the experiments. Similarly, knocking out MINK1 induced 5FU mediated cell death in chemoresistant cells (Fig. 2D). Enhanced p-H2AX and cleaved PARP was observed in MINK1KO cells followed by treatment with 5FU indicating the potential role of MINK1 in mediating 5FU resistance (Fig. 2E,F). Further, to test the in vivo efficacy of the kinome screening data, we implanted PDC2 MINK1WT cells into right upper flank and PDC2 MINK1KO cells into the left upper flank of nude mice followed by treatment with 5FU. Treatment with 5FU (10 mg/kg) significantly reduced the tumor burden in the MINK1KO but not in MINK1WT group (Fig. 2G-I). Immunohistochemistry data suggests markedly decreased cell proliferation signal (Ki67) in 5FU-treated MINK1KO tumors (Fig. 2J). Earlier it is known that

selective knockdown of MINK1 decreases the migration of human breast cancer lines (*10*). To evaluate whether depletion of MINK1 also reduces migration of chemoresistant OSCC lines and PDC2, Boyden chamber assays and scratch/wound healing assays were performed. The data suggest that knock out of MINK1 followed by treatment with 5FU significantly reduces the relative number of migrated cells (Fig. S6A). Similarly, scratch area analysis suggest that percentage of scratch area is significantly higher when 5FU is treated to MINK1KO drug resistant cells (Fig. S6 B, C). These data indicate MINK1 dependency of 5FU resistant OSCC.

Ectopic expression of MINK1 promotes 5FU resistance in OSCC: To confirm the potential role of MINK1 in 5FU resistance, we performed gain of function study. For this, using a lentiviral approach we generated MINK1ShRNA stable clones in 5FUR lines and PDC2 (MINK1UTRKD), where the shRNA targets the 3'UTR of MINK1 mRNA. For ectopic overexpression of MINK1, the MINK1UTRKD cells were transfected with pDESTCMV/TO MINK1 vector (Fig. 3A). The cell viability and cell death data suggest that knocking down MINK1 in 5FUR cells result in sensitizing the resistant cells to 5FU, however ectopic overexpression of MINK1 rescues the 5FU resistant phenotype (Fig. 3B, C). Similarly, immunostaining data suggest enhanced p-H2AX signal in MINK1UTRKD cells, whereas ectopic overexpression of MINK1 reduces the p-H2AX signal indicating rescue of 5FU resistance in OSCC cells (Fig. 3D). We also observed the rescue of cleaved PARP with ectopic expression of MINK1 suggesting reduced cell death (Fig. 3E). Finally, when MINK1 was overexpressed in OSCC sensitive lines, cells showed resistance to 5FU induced cell death (Fig. 3F).

MINK1 downregulates the expression of p53 in chemoresistant OSCC through activation of AKT and MDM2. To understand the specific role of MINK1 in 5FU resistant OSCC, we performed high-throughput phosphorylation profiling with 1,318 site-specific antibodies from over 30 signaling pathways in 5FUR cells stably expressing MINK1KO and MINK1WT. From this study, phosphorylation of p53 at Ser33 and Ser15 were found to be significantly up regulated in MINK1KO cells as compared to MINK1WT cells. In addition to this, phosphorylation of AKT at Ser473 and phosphorylation of MDM2 at Ser166 were found to be down regulated in MINK1KO cells as compared to MINK1WT (Fig. 4A). Further, immunoblotting was performed to validate the finding of phosphorylation profiling antibody array. The data suggest that phosphorylation of p53 at Ser15 and Ser33 is significantly upregulated and phosphorylation of MDM2 at Ser166 is profoundly downregulated in MINK1KO cells as compared to MINK1WT chemoresistant cells (Fig. 4B). In addition, p53 was also found to be upregulated in MINK1KO cells (Fig. 4B). Next, when MINK1 was ectopically overexpressed in MINK1KD (shRNA targeting 3'UTR) clones, downregulation of p53, p-p53 (Ser33) and p-p53 (Ser15) were observed in chemoresistant OSCC lines (Fig. 4C). In harmony to our finding of phosphorylation array, p-AKT(Ser473) was found to be down regulated in MINK1 depleted cells, which was rescued with ectopic overexpression of MINK1 (Fig. 4 D, E). To confirm the potential role of AKT in modulating MINK1 mediated p53 regulation, we ectopically overexpressed constitutively active AKT (myrAKT) in MINK1KO cells. The immunoblotting data suggest that expression of p53, p-p53 (Ser33) and p-p53 (Ser15) were downregulated when MyrAKT was overexpressed in MINK1KO cells (Fig. 4F). Similarly, when MINK1 over expressing cells were treated with AKT inhibitor (Akti-1/2) , the p53 expression was rescued along with downregulation of p-MDM2

(Ser166) (Fig. 4G). p53 target genes were also evaluated in MINK1 KO cells and the immunoblotting data suggest that expression of p21, NOXA and TIGAR in MINK1KO clones were upregulated as compared to MINK1WT clones (Fig. 4H).

Evaluation of Lestaurtinib as MINK1 inhibitor to reverse 5FU resistance in OSCC: From the screening data, we observed that MINK1 expression is elevated in chemoresistant OSCC and genetic inhibition of the same sensitizes drug resistant lines to 5FU induced cell death. Hence, MINK1 can be a potential therapeutic target to overcome chemoresistance in OSCC. Very limited information on the inhibitors of MINK1 is available in the literature. Hence, we looked for the potential MINK1 inhibitors in the international union of basic and clinical pharmacology (IUPHAR) database, where a screen of 72 inhibitors against 456 human kinases binding activity is provided. Among the potential twelve MINK1 inhibitors, we tested the MINK1 inhibitory activity of three inhibitors i.e., staurosporine, pexmetinib and lestaurtinib. The kinase assay data suggest that lestaurtinib and pexametinib have highest inhibitory activity for MINK1 (Fig. 5A). The 50% MINK1 inhibitory activity was observed at concertation of 100 nM in case of lestaurtinib and 10 µM for pexmetinib (Fig. 5B). Next, cell viability assay was performed to select a dose of lestaurtinib and pexmetinib that does not affect cell viability when treated alone (viability > 80%) in 5FU resistant OSCC lines (Fig. 5C, D). Further, the cell viability and cell death data suggest that the selected sub lethal dose of lestaurtinib (50nM) and pexmetinib (500µM) can efficiently restore 5FU mediated cell death in chemoresistant OSCC lines and PDC2 (Fig. 5 E, F). The IC50 value of 5FU in H3575FUR is 20.49µM, however combination of lestaurtinib (50nM) decreases the IC50 value to 4.82 µM and combination of pexmetinib (500µM) lowers the IC50 value of 5FU to 7.08 µM (Fig. 5E). As lestaurtinib, with a much lower concentration (50nM) as compared to pexmetinib (500nM) sensitize 5FU to chemoresistant cells, from here on lestaurtinib was considered for rest of the study. Enhanced expression of p-H2AX and cleaved PARP was observed only in combination group with lestaurtinib and 5FU indicating programmed cell death (Fig. 5G, H). Further, we found that lestaurtinib failed to sensitize 5FU mediated cell death in MINK1 knocked out 5FUR lines (Fig. 5I), which suggests that lestaurtinib conferred 5FU sensitivity by inhibiting MINK1 kinase activity. To check the in vivo efficacy of this novel combination, nude mice xenograft model was performed using patient derived cells (PDC2). The in vivo data suggest that the combination of lestaurtinib (20mg/kg) and 5FU (10mg/kg) profoundly reduced the tumor burden as compared to treatment with either of the single agents (Fig. 6A-C). Immunohistochemistry data suggest significant reduction in CD44 and Ki67 expression along with increased expression of cleaved caspase 3 in combination group (Fig. 6D). Finally, we performed combinatorial anti-tumor effect of non-cytotoxic extremely low dose of cisplatin (1µM), 5FU (1µM) and lestaurtinib (50nM) in PDC2. The cell viability, cell death, western blotting and colony forming assay data suggest significantly higher cell death in cisplatin, 5FU and lestaurtinib combinatorial group, as compared to any other possible combinatorial group, i.e. 5FU and lestaurtinib or cisplatin and lestaurtinib or cisplatin and 5FU (Figure S8).

Discussion: The hallmark chemoresistant phenotypes of cancer cells are reduced apoptosis, altered metabolic activity, enhanced cancer stem cells like population, increased drug efflux and decreased drug accumulations. However, the causative factors which are responsible for acquired chemoresistance is largely not known. It is well known that kinases play key role in various

processes of carcinogenesis and kinase inhibitors are established as potential anti-tumor agents. In this study, for the first time, we have performed a kinome screening in drug resistant cancer cells to explore the potential kinase(s) those mediate 5FU resistance in OSCC. From the primary and secondary kinome screening, MINK1 was found to be top ranked kinase that can re-sensitize drug resistant cells to 5FU. Overall, MINK1 is known to regulate cell senescence, cell motility and migration. Till date the potential role of MINK1 in modulating chemoresistanace is still unknown. Here in this study, we found the novel function of MINK1 by which it regulates 5FU resistance in OSCC.

To understand the mechanism by which MINK1 regulates 5FU resistance, we performed a high-throughput phosphorylation profiling in 5FUR cells stably expressing MINK1sgRNA. From this study, we found p- p53 (Ser33) and p-53(Ser15) to be significantly up-regulated in MINK1KO cells and p-AKT (Ser473) and p-MDM2 (Ser166) were found to be down-regulated in MINK1KO cells as compared to MINK1WT. The tumor suppressor p53 is phosphorylated at various amino acids by different kinases, which tightly regulates its stability (*13*). It is well known that MDM2 (a E3 ubiquitin ligase) acts as a negative regulator of p53. MDM2 forms a complex with p53 and facilitates the recruitment of ubiquitin molecules for its degradation (*14*). Earlier, it was established that insulin induced activated AKT (Ser473) phosphorylates MDM2 at Ser 166 and Ser 186, which can lead to MDM2 mediated proteasomal degradation of p53 in cytoplasm as well as in nucleus (*15, 16*). These events lead to blocking of p53-mediated transcription of genes those generally involve in apoptosis, cell cycle regulation and senescence. In addition to this, p53 is phosphorylated at Ser15 by ATM, DNA-PK and ATR in response to DNA damage (*17-19*). Hence, phosphorylation of Ser15 and Ser33 leads to activation and stabilization of p53 as they attenuate the MDM2 mediated degradation of p53 (*20, 21*). Overall, in this study we found that MINK1 regulates the expression of p53 through activation of AKT which in turns triggers p-MDM2 (Ser 166) (Figure 6 E).

Jin et al 2018 performed a kinome screening in cisplatin resistant cells to explore the potential kinases those confer cisplatin resistance in HNSCC. The data suggests that microtubule-associated serine/threonine-protein kinase 1 (MAST1) mediates cisplatin resistance in HNSCC by phosphorylating MEK1, triggering cRaf-independent activation of MEK1, which led to down regulation of BH3 only protein BIM. Jin et al 2018 also found that lestaurtinib to be a potent inhibitor of MAST1. Lestaurtinib successfully restores the cisplatin induced cell death in cisplatin resistant cells (*6*). Lestaurtinib not only inhibits MAST1 activity but also known as an inhibitor of JAK2, Trk and FLT3 (*22, 23*). In this study, we found that lestaurtinib inhibits activity of MINK1 and lestaurtinib can resensitize the drug resistant OSCC to 5FU. The most common chemotherapy regimen for OSCC is the combination of cisplatin, 5FU and Docetaxel (TPF). Finally, our data suggests that combination of extremely low dose of cisplatin (1μM), 5FU (1μM) and lestaurtinib (50nM) can overcome chemoresistance in OSCC (Fig. S8). Currently lestaurtinib alone or in combination with other chemotherapy drug is under clinical investigation (phase II) for patients having AML and it is well tolerated in human beings (*24*).

One of the limitations in this study include small size of clinical samples for validation of targets obtained from kinome screening. Determining expression of MINK1 in the tumor of large cohort

of responders and non-responders would enable us to determine if MINK1 expression can be a predictor of 5FU response in advanced OSCC. Besides this, though we have demonstrate that MINK1 negatively regulates P53 through AKT/MDM2 axis in 5FU resistance OSCC, the 5FU specificity of this MINK1 driven signalling cascade remains to be fully elucidated.

Overall, our data suggests that MINK1 is a mediator of 5FU resistance in OSCC. MINK1 regulates the expression of p53 in chemoresistant cells and genetic or pharmacological (Lestaurtinib) inhibition of MINK1 successfully resensitized chemoresistant lines to 5FU. This novel combination of 5FU and Lestaurtinib needs further clinical investigation.

Materials and Methods

Study design: This study is designed to explore the potential kinase (s) those modulate 5FU resistance in OSCC and to evaluate the preclinical efficacy of inhibitor against the target kinase, which will overcome chemoresistance in OSCC. This objective was achieved by I) performing a CRISPR/Cas9 based kinome screening to find out the kinase(s), which can be targeted to resensitize chemoresistant cells to 5FU, II) exploring the mechanism by which the kinase modulates 5FU resistance, III) to explore a kinase inhibitor against the target kinase found from screening and IV) to evaluate if the kinase inhibitor can improve the response to chemotherapy in chemoresistant OSCC both in vitro and in preclinical animal models.

Cell culture: The human tongue OSCC lines **(**H357, SCC4 and SCC9) were obtained from Sigma Aldrich, sourced from European collection of authenticated cell culture. All OSCC cell lines were cultured and maintained in DMEM F12 supplemented with 10% FBS (Thermo Fisher Scientific), penicillin–streptomycin (Pan Biotech) and 0.5 ug/ml sodium hydrocortisone succinate. HEK 293T cells were maintained in DMEM supplemented with 10% FBS and penicillin–streptomycin (Pan Biotech).

Generation of 5-Fluorouracil resistant cell lines: For establishment of 5FU resistant cell lines, human OSCC cell lines (H357, SCC4 and SCC9) were initially treated with 1μM (lower dose) of 5-Fluorouracil for a week and then the concentration of 5FU was gradually increased up to the IC50 value, i.e. 10 μM for H357, 15 μM for SCC4 and 7.5 μM for SCC9 within a span of 3 months. Parental cells were grouped as sensitive (H357 5FUS, SCC4 5FUS and SCC9 5FUS) and after a period of 8 months of 5FU treatment, they were termed as 5FU Resistant (H357 5FUR, SCC4 5FUR and SCC9 5FUR) cells.

High Content Screening: 1000 cells/ well were seeded in black flat bottom 96 well plate (Thermo Scientific™ Nunc) and divided into two experimental groups, one without 5FU treatment and the other with 5FU treatment. A CRISPR based kinome-wide screening was performed using a lentiviral sgRNA library (LentiArray™ Human Kinase CRISPR Library, Thermo Fisher Scientific, M3775) that knocks out 840 kinase and kinase related genes individually with total

number of 3214 sgRNA constructs. Transduction of lentiviruses (MOI:2) containing pooled sg RNAs (up to 4) targeting each of 840 genes along with positive and negative control lentiviruses into individual wells was carried out in presence of polybrene (8µg/ml). At 48 hours post transduction, selection with puromycin (0.5µg/ml) was performed for next 2-3 days, followed by treatment of vehicle control and 5FU at sub lethal dose respectively in both groups for 48h. Finally, cells were stained with LIVE/DEAD™ Viability/Cytotoxicity Kit (Thermo Fisher Scientific Cat # L3224) and high content screening was performed using CellInsight CX7 High-Content Screening (HCS) Platform. The green fluorescence indicates the living cells and red fluorescence indicates dead cells. Images from 20 fields per well were acquired using 10X objective lens. Two different fluorescent channels (excitation wavelengths -488nm and 561nm) were used for acquiring images. Image analysis was performed using the HCS Studio software. A threshold value for each channel was set once and used for the entire screening. To identify the cells, segmentation was done. Some of the clumped and poorly segmented cells were excluded from further analysis on the basis of area, shape and intensity. On the basis of intensity, number of live and dead cells were counted and an objective mask (blue lines in the images) was created around each cell. For positive control, Cas9 over expressing cells were transduced with lentiviruses expressing sgRNA targeting human hypoxanthine phosphoribosyltransferase 1 (HPRT1) (LentiArray™ CRISPR Positive Control Lentivirus, human HPRT, Thermo Fisher Scientific Cat # A32829). HPRT1 knockout cells shows resistance to 6-thioguanine (6TG) induced cell death. For negative control, Cas9 over expressing cells were transduced with lentiviruses expressing gRNA with no sequence homology to any region of the human genome (LentiArray™ CRISPR Negative Control Lentivirus, Thermo Fisher Scientific, Cat # A32327).

Genomic Cleavage Detection Assay: The genomic cleavage efficiency was measured using the GeneArt® Genomic Cleavage Detection kit (Thermo Fisher Scientific, Cat # A24372). For this, cells were lysed and DNA was extracted, followed by PCR amplification of the region on genome, where Cas9 endonuclease introduced a cleavage, using specifically designed primers as described in the protocol of the kit. Further, the PCR products were denatured and allowed for random reannealing, so that mismatches are generated as a result of genomic insertions or deletions (indels) created by the cellular repair mechanisms following the cleavage induced by Cas9. These mismatches were subsequently detected and cleaved by Detection Enzyme and then the resultant bands were analyzed by agarose gel electrophoresis. Primers used in this study for cleavage detection assay are mentioned in Table S2.

Lentivirus production and generation of stable MINK1 KO cell lines : LentiCas9-Blast was obtained from addgene (#52962) which is kindly deposited by Feng Zhang lab (*25*). sgRNAs targeting MINK1 were cloned into pKLV2-U6gRNA5(BbsI)-PGKpuro2ABFP-W (Addgene #67974) vector as per the protocol mentioned in addgene, which is kindly deposited by Kosuke Yusa lab (*26*). Respective lentiviruses were produced by transfection of LentiCas9-Blast or pKLV2-U6gRNA5(BbsI)-PGKpuro2ABFP-W plasmid along with packaging plasmid psPAX2 and envelop plasmid pMD2G into HEK293T cells as described in Shriwas et al (*27*). Further 5FUR cells were infected with MINK1 sgRNA lentivirus using polybrene (8µg/ml) followed by puromycin (up to 5µg/ml) selection. After a week cells were picked up and seeded in 96 well plates

with 1 cell/well dilution. Confirmations were done by western analysis. All sgRNA sequences used in this study are mentioned in Table S2.

Lentivirus production and generation of stable MINK1 KD cell lines: pLKO.1vector was obtained from addgene (Cat #10878), which is kindly deposited by David Root lab (*28*). shRNAs targeting MINK1 were cloned into pLKO.1vector as per the protocol mentioned in addgene. Lentivirus was produced by transfection of pLKO.1 plasmid along with packaging plasmid psPAX2 and envelop plasmid pMD2G into HEK293T cells. Further 5FUR cells were infected with MINK1 shRNA lentivirus using polybrene (8µg/ml) followed by puromycin (up to 5µg/ml) selection. After 15 days colonies were picked up and confirmations were done by western analysis. All shRNA sequences used in this study are mentioned in Table S2.

RT-PCR and Real Time Quantitative PCR: RNA mini kit (Himedia, Cat# MB602) was used to isolate total RNA as per manufacturer's instruction and quantified by Nanodrop. Verso cDNA synthesis kit (ThermoFisher Scientific, Cat # AB1453A) was used to synthesize c-DNA by reverse transcription PCR using 300 ng of RNA. qRT-PCR was carried out using SYBR Green master mix (Thermo Fisher scientific Cat # 4367659). GAPDH was used as a loading control. The primers (oligos) sequence used for qRT-PCR in this study are listed in Table S2.

Immunoblotting: Immunoblotting was performed by loading equal amounts of cell lysates as described earlier (*29*). In this study, primary antibodies used were against β-actin (Sigma, Cat#A2066), Cas9 (CST, Cat #14697S), MINK1 (Sigma, Cat# HPA056296, Invitrogen, Cat# PA5-28901), P53 (CST, Cat #2527T), p-P53(Ser15) (CST, Cat #9284T), p-P53(Ser33) (CST, Cat #2526), PARP (CST, Cat #9542L), p^{s-139}-H2AX (CST, Cat # 9718S), AKT (CST, Cat #9272S), pAKT(Ser473) (CST, Cat #4058S), MDM2 (Santa Cruz, Cat #sc965), pMDM2 (ser166) (Abcam, Cat # ab131355), TIGAR (Abcam, Cat # Ab37910), P21(CST, Cat # 2947S), NOXA (Imgenex, Cat # IMG-349A).

Assessment of cell viability: Cell viability was measured by 3-(4, 5-dimethylthiazol-2-yl)-2, 5-diphenyltetrazolium bromide (MTT; Sigma-Aldrich) assay as per manufacturer's instruction.

Colony formation assay: Colony formation assay was performed as described in Shriwas et al (*30*).

Annexin-V PE/7-AAD Assay: Apoptosis and cell death assay was performed by using Annexin V Apoptosis Detection Kit PE (eBioscience™, USA, Cat # 88-8102-74) as described earlier (*30*) and cell death was monitored using a flow cytometer (BD FACS Fortessa, USA).

Immunofluorescence: The cells were seeded on lysine coated coverslip and cultured for overnight. On next day, cells were treated with 5FU for 48 hrs followed by 4% formaldehyde fixation for 15 mins. Next, cells were permeabilized with 1 × permeabilization buffer (eBioscience 00-8333-56) for 45 mins, followed by blocking with 3% BSA for 1 h at room temperature. After which, the cells were incubated with primary antibody overnight at 4 °C, washed three times with PBST pH 8.0 followed by 1hr incubation with Goat anti–Rabbit IgG(H+L) secondary Antibody, Alexa Fluor® 488 conjugate (Invitrogen, Cat #A -11008). After washing three times with PBST pH 8.0, cells were mounted with DAPI (Slow Fade ® GOLD Antifade, Thermo Fisher Scientific,

Cat # S36938). Images were captured using a confocal microscopy (LEICA TCS-SP8). Anti p^{S-139}-H2AX (CST, Cat # 9718S) primary antibody was used for this study.

Immunohistochemistry: Immunohistochemistry of formalin fixed paraffin-embedded samples (OSCC patients' tumors and Xenograft tumors from mice) were performed as described previously (*31*). Antibodies against MINK1 (Sigma, Cat# HPA056296, Invitrogen, Cat# PA5-28901), CD44 (NOVUS, Cat# NBP1-31488), Cleaved Caspase-3 (CST, Cat# 9661S), Ki67 (Vector, Cat #VPRM04) were used for IHC. Images were obtained using Leica DM500 microscope. Q-score was calculated by multiplying percentage of positive cells with staining (P) and intensity of staining (I). P was determined by the percentage of positively stained cells in the section and I was determined by the intensity of the staining in the section i.e. strong (value=3), intermediate (value=2), weak (value=1) and negative (value=0).

Patient Derived Xenograft: BALB/C-nude mice (6-8 weeks, male, NCr-Foxn1nu athymic) were purchased from Hylasco Bio-Technology Pvt. Ltd. For xenograft model early passage of patient-derived cells (PDC2) established from chemo non-responder patient (treated with TPF without having any response) was considered. Two million cells were suspended in phosphate-buffered solution-Matrigel (1:1, 100 µl) and transplanted into upper flank of mice. The PDC MINK1WT cells were injected in right upper flank and PDC MINK1KO cells were injected in the left upper flank of same mice. These mice were randomly divided into 2 groups (n=5) once the tumors reached a volume of 50 mm^3 and injected with vehicle control or 5FU (10mg/kg) intraperitonially twice a week. In another experimental set up, PDC2 WT cells were injected in right upper flank of mice. These mice were randomly divided into 4 groups (n=5) after the tumors have reached a volume of 50 mm^3 and injected with vehicle control, 5FU (10mg/kg), Lestaurtinib (20mg/kg) and 5FU (10mg/kg) and Lestaurtinib (20mg/kg) respectively in each individual group, intraperitonially twice a week. Tumor size was measured using digital Vernier caliper twice a week until the completion of experiments. Tumor volume was determined using the following formula: Tumor volume (mm^3) = $(\text{minimum diameter})^2 \times (\text{maximum diameter})/2$.

Transient transfection and overexpression of MINK1 and myr-AKT in MINK1 KD cell lines: pDONR223-MINK1 (Plasmid #23522) was procured from addgene followed by transfer of the insert into pLenti CMV/TO Puro DEST (670-1) (Addgene, Cat#17293) destination vector by gateway cloning method using Gateway LR Clonase II Plus Enzyme mix (Invitrogen, Cat# 1756069). These plasmids were kindly deposited by William Hahn, David Root labs (*32*) and Eric Campeau, Paul Kaufman labs (*33*) in addgene. Further, MINK1 knockdown cells, stably expressing shRNA#1 targeting 3' UTR of MINK1 mRNA, were transiently transfected with pLenti CMV/TO Puro DEST-MINK1 using the ViaFect transfection reagent (Promega Cat# E4982). The transfection efficiency was confirmed by immunoblotting against Anti-MINK1. pLNCX myr HA Akt1 (Addgene, Cat #9005) was used for transient overexpression of constitutively activated AKT. The myr HA Akt1 vector was kindly deposited to Addgene by Sellers WR lab (*34*).

OSCC patient sample: Loco regionally advanced OSCC samples were collected. Neoadjuvant chemotherapy has been prescribed before surgery and/or radiotherapy. The three-drug combination of TPF is having highest response (TAX 324). After chemotherapy (CT) the response is evaluated as per RECIST criteria (Response evaluation criteria in solid tumors) by clinical and

radiological evaluation. After chemotherapy the patient can be grouped as complete response (CR), Partial Response (PR), stable disease (SD) or Progressive Disease (PD). If there was no evidence of malignancy, then it was diagnosed as complete response (CR). If the target lesions had decreased more than equal to 30% of the sum of the longest diameter, then it was diagnosed as partial response (PR). If there was no sign of either CR or PR, then it was called stable disease, and if the target lesions had increased more than or equal to 20% of the sum of the longest diameter, then it was called PD (progressive disease). As the patients showing CR and PR have responded to the CT they are categorized as Responders and the patients with stable disease or PD with almost no response to CT are categorized as Non-Responders. Human Ethics Committee (HEC) of the Institution of Life Sciences approved all patient-related studies, and informed consent was obtained from all patients. Study subject details with treatment modalities are presented in Table S1a and b.

Phospho-Protein Profiling: For performing the Phospho Explorer Antibody Array (Full Moon Biosystems Cat# PEX10), $5X10^6$ number of H3575FUR MINK1WT and H3575FUR MINK1KO cells were seeded and lysates were isolated, after which the protein samples were labelled with biotin as described by manufacturer. Biotinylated protein samples were further blocked in skim milk and were subjected to coupling with the 1318 number of antibodies present on the array slides. Then for the detection of expression of phospho proteins, Cy3-streptavidin (Sigma, Cat#S6402) was added. Array slides were scanned at Fullmoon Biosystems array scanning service and the image analysis was done using ImageJ software.

***In vitro* MINK1 kinase activity assays:** MINK1 Kinase Enzyme System (Promega Cat No# V3911) and ADP-Glo™ Kinase Assay (Promega Cat No#V9101) were procured to perform the *in vitro* kinase assay. Selected compounds (10 μM) were incubated at room temperature for 1 hr with recombinant human MINK1 kinase along with substrate MBP and ATP to perform the kinase reaction using 1X kinase buffer. Further ADP-Glo™ Reagent was added at room temperature for 40 mins to stop the kinase reaction and deplete the unconsumed ATP, hence leaving only ADP. Then Kinase detection reagent was added and incubated at room temperature for 30 mins to convert ADP to ATP and introduce luciferase and luciferin to detect ATP. Finally, the luminescence was measured using VICTOR® Nivo™ Multimode Plate Reader (Perkin Elmer).

Trans-well migration assay

For trans-well migration assay, MINK1WT and MINK1 KO chemoresistant cells were treated with vehicle control or 5FU (10 μM, 48hrs). In another experimental set up, 5FU resistant cells were treated with vehicle control, 5FU (10 μM), Lestaurtinib (50 nM), or 5FU (10 μM) and Lestaurtinib (50 nM). After treatment, cells were seeded at a density of 1×10^4 cells in the upper chamber of 24-well trans-well system in 250 μL of serum free DMEM-F12 medium. 750 μL of DMEM-F12 Medium supplemented with 10% serum, used as a chemo-attractant, was added in the lower chamber. After 24 hrs of incubation, the cells inside the upper chamber were scrubbed with a cotton swab, whereas the migrated cells were fixed and stained with crystal violet, followed by quantification of migration by manual counting using a microsope.

***In vitro* scratch assay:** *In vitro* scratch assay was performed as described earlier (*29*).

Statistical analysis: All data points are presented as mean and standard deviation and Graph Pad Prism 9.0 was used for calculation. The statistical significance was calculated by one-way variance (one-way ANOVA), Two-Way ANOVA and considered significance at $P \leq 0.05$.

Study approval: This study was approved by the Institute review Board and Human Ethics committees (HEC) of Institute of Life Sciences, Bhubaneswar (110/HEC/21) and All India Institute of Medical Sciences (AIIMS), Bhubaneswar (T/EMF/Surg.Onco/19/03). The animal related experiments were performed in accordance to the protocol approved by Institutional Animal Ethics Committee of Institute of Life Sciences, Bhubaneswar (ILS/IAEC-204-AH/DEC-20). Approved procedures were followed for patient recruitment and after receiving written informed consent from each patient, tissues samples were collected. Institutional biosafety committee (IBSC) approved all related experiments.

Supplementary Materials

Figure S1: Characterization of sensitive and 5FU resistant OSCC lines

Figure S2: Overexpression of Cas9 in 5FU resistant OSCC lines and PDC:

Figure S3: Characterization of Cas9 overexpressing OSCC lines regarding 5FU resistance, polybrene tolerance and puromycin sensitivity

Figure S4: Validation of 5FU resistance and optimization of kinome screening conditions using high content analyzer

Figure S5: Secondary screening identifies MINK1 as a common target among different 5FU resistant OSCC lines

Figure S6: MINK1 genomic ablation negatively affects tumor cell migration in OSCC

Figure S7: Lestaurtinib negatively affects tumor cell migration in OSCC

Figure S8: Evaluation of combinatorial anti-tumor effect of low dose cisplatin, 5FU and lestaurtinb in TPF resistant patient derived cells (PDC2).

Acknowledgements:. PM is a CSIR-SRF, SM is UGC-SRF, SAA is a UGC-JRF.

Funding: Grant support: This work is supported by ICMR (5/13/9/2019-NCD-III), Institute of Life Sciences, Bhubaneswar intramural support and DBT BT/ INF/22/SP28293/2018 (for imaging facility).

Author contribution

SM, PM, OS, MP, SAA and SP performed experiments, and analyzed the data, under the direction of R.D. RR, MS and S.K.M. performed part of experiments. SM, PM and R.D. designed experiments and supervised the study. R.D wrote the manuscript. All authors approved the final version.

Competing interests: The authors declare no conflict of interest.

References

1. D. E. Johnson, B. Burtness, C. R. Leemans, V. W. Y. Lui, J. E. Bauman, J. R. Grandis, Head and neck squamous cell carcinoma. *Nat Rev Dis Primers* **6**, 92 (2020).
2. A. Chaturvedi, N. Husain, S. Misra, V. Kumar, S. Gupta, N. Akhtar, M. Lakshmanan, S. Garg, A. Arora, K. Jain, Validation of the Brandwein Gensler Risk Model in Patients of Oral Cavity Squamous Cell Carcinoma in North India. *Head Neck Pathol* **14**, 616-622 (2020).
3. S. Vishak, B. Rangarajan, V. D. Kekatpure, Neoadjuvant chemotherapy in oral cancers: Selecting the right patients. *Indian journal of medical and paediatric oncology : official journal of Indian Society of Medical & Paediatric Oncology* **36**, 148-153 (2015).
4. S. Maji, S. Panda, S. K. Samal, O. Shriwas, R. Rath, M. Pellecchia, L. Emdad, S. K. Das, P. B. Fisher, R. Dash, Bcl-2 Antiapoptotic Family Proteins and Chemoresistance in Cancer. *Advances in cancer research* **137**, 37-75 (2018).
5. S. Gross, R. Rahal, N. Stransky, C. Lengauer, K. P. Hoeflich, Targeting cancer with kinase inhibitors. *J Clin Invest* **125**, 1780-1789 (2015).
6. L. Jin, J. Chun, C. Pan, D. Li, R. Lin, G. N. Alesi, X. Wang, H. B. Kang, L. Song, D. Wang, G. Zhang, J. Fan, T. J. Boggon, L. Zhou, J. Kowalski, C. K. Qu, C. E. Steuer, G. Z. Chen, N. F. Saba, L. H. Boise, T. K. Owonikoko, F. R. Khuri, K. R. Magliocca, D. M. Shin, S. Lonial, S. Kang, MAST1 Drives Cisplatin Resistance in Human Cancers by Rewiring cRaf-Independent MEK Activation. *Cancer cell* **34**, 315-330 e317 (2018).
7. T. M. Brand, M. Iida, A. P. Stein, K. L. Corrigan, C. M. Braverman, N. Luthar, M. Toulany, P. S. Gill, R. Salgia, R. J. Kimple, D. L. Wheeler, AXL mediates resistance to cetuximab therapy. *Cancer research* **74**, 5152-5164 (2014).
8. T. Rampias, A. Giagini, S. Siolos, H. Matsuzaki, C. Sasaki, A. Scorilas, A. Psyrri, RAS/PI3K crosstalk and cetuximab resistance in head and neck squamous cell carcinoma. *Clin Cancer Res* **20**, 2933-2946 (2014).
9. I. Dan, N. M. Watanabe, T. Kobayashi, K. Yamashita-Suzuki, Y. Fukagaya, E. Kajikawa, W. K. Kimura, T. M. Nakashima, K. Matsumoto, J. Ninomiya-Tsuji, A. Kusumi, Molecular cloning of MINK, a novel member of mammalian GCK family kinases, which is up-regulated during postnatal mouse cerebral development. *FEBS Lett* **469**, 19-23 (2000).
10. A. M. Daulat, F. Bertucci, S. Audebert, A. Serge, P. Finetti, E. Josselin, R. Castellano, D. Birnbaum, S. Angers, J. P. Borg, PRICKLE1 Contributes to Cancer Cell Dissemination through Its Interaction with mTORC2. *Developmental cell* **37**, 311-325 (2016).
11. Y. C. Su, J. E. Treisman, E. Y. Skolnik, The Drosophila Ste20-related kinase misshapen is required for embryonic dorsal closure and acts through a JNK MAPK module on an evolutionarily conserved signaling pathway. *Genes Dev* **12**, 2371-2380 (1998).
12. S. Maji, O. Shriwas, S. K. Samal, M. Priyadarshini, R. Rath, S. Panda, S. K. Das Majumdar, D. K. Muduly, R. Dash, STAT3- and GSK3beta-mediated Mcl-1 regulation modulates TPF resistance in oral squamous cell carcinoma. *Carcinogenesis* **40**, 173-183 (2019).
13. N. J. Maclaine, T. R. Hupp, The regulation of p53 by phosphorylation: a model for how distinct signals integrate into the p53 pathway. *Aging (Albany NY)* **1**, 490-502 (2009).
14. U. M. Moll, O. Petrenko, The MDM2-p53 interaction. *Mol Cancer Res* **1**, 1001-1008 (2003).
15. T. M. Gottlieb, J. F. Leal, R. Seger, Y. Taya, M. Oren, Cross-talk between Akt, p53 and Mdm2: possible implications for the regulation of apoptosis. *Oncogene* **21**, 1299-1303 (2002).
16. L. D. Mayo, D. B. Donner, A phosphatidylinositol 3-kinase/Akt pathway promotes translocation of Mdm2 from the cytoplasm to the nucleus. *Proc Natl Acad Sci U S A* **98**, 11598-11603 (2001).

17. K. K. Khanna, K. E. Keating, S. Kozlov, S. Scott, M. Gatei, K. Hobson, Y. Taya, B. Gabrielli, D. Chan, S. P. Lees-Miller, M. F. Lavin, ATM associates with and phosphorylates p53: mapping the region of interaction. *Nat Genet* **20**, 398-400 (1998).
18. N. D. Lakin, B. C. Hann, S. P. Jackson, The ataxia-telangiectasia related protein ATR mediates DNA-dependent phosphorylation of p53. *Oncogene* **18**, 3989-3995 (1999).
19. S. Y. Shieh, M. Ikeda, Y. Taya, C. Prives, DNA damage-induced phosphorylation of p53 alleviates inhibition by MDM2. *Cell* **91**, 325-334 (1997).
20. K. Sakaguchi, J. E. Herrera, S. Saito, T. Miki, M. Bustin, A. Vassilev, C. W. Anderson, E. Appella, DNA damage activates p53 through a phosphorylation-acetylation cascade. *Genes Dev* **12**, 2831-2841 (1998).
21. S. Yogosawa, K. Yoshida, Tumor suppressive role for kinases phosphorylating p53 in DNA damage-induced apoptosis. *Cancer Sci* **109**, 3376-3382 (2018).
22. E. O. Hexner, C. Serdikoff, M. Jan, C. R. Swider, C. Robinson, S. Yang, T. Angeles, S. G. Emerson, M. Carroll, B. Ruggeri, P. Dobrzanski, Lestaurtinib (CEP701) is a JAK2 inhibitor that suppresses JAK2/STAT5 signaling and the proliferation of primary erythroid cells from patients with myeloproliferative disorders. *Blood* **111**, 5663-5671 (2008).
23. M. Shabbir, R. Stuart, Lestaurtinib, a multitargeted tyrosine kinase inhibitor: from bench to bedside. *Expert Opin Investig Drugs* **19**, 427-436 (2010).
24. S. Knapper, A. K. Burnett, T. Littlewood, W. J. Kell, S. Agrawal, R. Chopra, R. Clark, M. J. Levis, D. Small, A phase 2 trial of the FLT3 inhibitor lestaurtinib (CEP701) as first-line treatment for older patients with acute myeloid leukemia not considered fit for intensive chemotherapy. *Blood* **108**, 3262-3270 (2006).
25. N. E. Sanjana, O. Shalem, F. Zhang, Improved vectors and genome-wide libraries for CRISPR screening. *Nat Methods* **11**, 783-784 (2014).
26. K. Tzelepis, H. Koike-Yusa, E. De Braekeleer, Y. Li, E. Metzakopian, O. M. Dovey, A. Mupo, V. Grinkevich, M. Li, M. Mazan, M. Gozdecka, S. Ohnishi, J. Cooper, M. Patel, T. McKerrell, B. Chen, A. F. Domingues, P. Gallipoli, S. Teichmann, H. Ponstingl, U. McDermott, J. Saez-Rodriguez, B. J. P. Huntly, F. Iorio, C. Pina, G. S. Vassiliou, K. Yusa, A CRISPR Dropout Screen Identifies Genetic Vulnerabilities and Therapeutic Targets in Acute Myeloid Leukemia. *Cell Rep* **17**, 1193-1205 (2016).
27. O. Shriwas, R. Arya, S. Mohanty, P. Mohapatra, S. Kumar, R. Rath, S. R. Kaushik, F. Pahwa, K. C. Murmu, S. K. D. Majumdar, D. K. Muduly, A. Dixit, P. Prasad, R. K. Nanda, R. Dash, RRBP1 rewires cisplatin resistance in oral squamous cell carcinoma by regulating Hippo pathway. *Br J Cancer* **124**, 2004-2016 (2021).
28. J. Moffat, D. A. Grueneberg, X. Yang, S. Y. Kim, A. M. Kloepfer, G. Hinkle, B. Piqani, T. M. Eisenhaure, B. Luo, J. K. Grenier, A. E. Carpenter, S. Y. Foo, S. A. Stewart, B. R. Stockwell, N. Hacohen, W. C. Hahn, E. S. Lander, D. M. Sabatini, D. E. Root, A lentiviral RNAi library for human and mouse genes applied to an arrayed viral high-content screen. *Cell* **124**, 1283-1298 (2006).
29. S. K. Samal, S. Routray, G. K. Veeramachaneni, R. Dash, M. Botlagunta, Ketorolac salt is a newly discovered DDX3 inhibitor to treat oral cancer. *Scientific reports* **5**, 9982 (2015).
30. O. Shriwas, M. Priyadarshini, S. K. Samal, R. Rath, S. Panda, S. K. Das Majumdar, D. K. Muduly, M. Botlagunta, R. Dash, DDX3 modulates cisplatin resistance in OSCC through ALKBH5-mediated m(6)A-demethylation of FOXM1 and NANOG. *Apoptosis* **25**, 233-246 (2020).
31. P. Mohapatra, O. Shriwas, S. Mohanty, A. Ghosh, S. Smita, S. R. Kaushik, R. Arya, R. Rath, S. K. Das Majumdar, D. K. Muduly, S. K. Raghav, R. K. Nanda, R. Dash, CMTM6 drives cisplatin resistance by regulating Wnt signaling through the ENO-1/AKT/GSK3beta axis. *JCI Insight* **6**, (2021).
32. C. M. Johannessen, J. S. Boehm, S. Y. Kim, S. R. Thomas, L. Wardwell, L. A. Johnson, C. M. Emery, N. Stransky, A. P. Cogdill, J. Barretina, G. Caponigro, H. Hieronymus, R. R. Murray, K. Salehi-

Ashtiani, D. E. Hill, M. Vidal, J. J. Zhao, X. Yang, O. Alkan, S. Kim, J. L. Harris, C. J. Wilson, V. E. Myer, P. M. Finan, D. E. Root, T. M. Roberts, T. Golub, K. T. Flaherty, R. Dummer, B. L. Weber, W. R. Sellers, R. Schlegel, J. A. Wargo, W. C. Hahn, L. A. Garraway, COT drives resistance to RAF inhibition through MAP kinase pathway reactivation. *Nature* **468**, 968-972 (2010).

33. E. Campeau, V. E. Ruhl, F. Rodier, C. L. Smith, B. L. Rahmberg, J. O. Fuss, J. Campisi, P. Yaswen, P. K. Cooper, P. D. Kaufman, A versatile viral system for expression and depletion of proteins in mammalian cells. *PloS one* **4**, e6529 (2009).

34. S. Ramaswamy, N. Nakamura, F. Vazquez, D. B. Batt, S. Perera, T. M. Roberts, W. R. Sellers, Regulation of G1 progression by the PTEN tumor suppressor protein is linked to inhibition of the phosphatidylinositol 3-kinase/Akt pathway. *Proc Natl Acad Sci U S A* **96**, 2110-2115 (1999).

Figure legends:

Figure 1: CRISPR based Kinome screening revealed MINK1 as a potential mediator for 5FU resistance in OSCC. A) Schematic presentation of approach for CRSPR/Cas9 based kinome knockout screening to discover the potential kinase responsible for 5FU resistance in OSCC. **B-C)** Primary screening of 840 kinases was performed with sublethal dose of 5FU (8μM). The kinases (n=506 nos) whose knockout alone induced significantly higher cell death (> 30%) depicted in red were excluded. From the rest of the kinases (n=334 nos) depicted in green, the survival fraction (5FU treated/ Vehicle Control) was determined and top 60 candidates having lowest survival fraction were considered for secondary screening. **D)** For secondary screening with top 60 kinases, four cell lines were considered i.e., H357 5FUR, SCC4 5FUR, SCC9 5FUR and H357CisR. After overlapping all three 5FUR cell lines, MINK1, SBK1, FKBP1A were found to be the common kinases among them. MINK1 was selected as a potential kinase target purely based on having the lowest survival fraction among all common candidates. **E)** The fluorescent images acquired from high content analyzer with indicated treated group during kinome screening. **F)** Lysates were collected from indicated cells and immunoblotting was performed with indicated antibodies. **G)** Protein expression of MINK1 was analyzed by IHC in chemotherapy- responder and chemotherapy-non-responder OSCC tumors. Scale bars: 50 μm. **H)** IHC scoring for MINK1 from panel G (Q Score =Staining Intensity × % of Staining), (Median, n=11 for chemotherapy-responder and n=23 for chemotherapy-non-responder) **P* < 0.05 by 2-tailed Student's t test. **I)** Protein expression of MINK1 was analyzed by immunohistochemistry (IHC) in pre- and post-TPF treated paired tumor samples from chemotherapy-non-responder patients. Scale bars: 50 μm. **J)** IHC scoring for MINK1 from panel I (Q Score =Staining Intensity × % of IHC Staining). **P* < 0.05 by 2-tailed Student's t test.

Figure 2: Selectively targeting MINK1 restores 5FU induced cell death in chemoresistant OSCC: A) MINK1 knock out clones were generated using a lentiviral approach expressing 2 different sgRNAs (#1 and #2) in Cas9 overexpressing 5FU resistant lines and PDC2. Immunoblotting was performed with indicated antibodies in indicated cells. Patient derived cells (PDC2) was established from tumor of TPF treated chemo-nonresponder patient. **B)** MINK1 KO and MINK1WT cells were treated with 5FU for 12 days and colony forming assays were performed as described in method section. Left panel: Bar diagram indicate the relative colony number (n=3 and *P < 0.05 by 2-way ANOVA). Right panel: representative photographs of colony

forming assay in each group. **C)** 5FU resistant cells stably expressing MINK1sgRNA (#1 and #2) and NTsgRNA were treated with 5FU for 48h and cell viability was determined by MTT assay (n=3 and 2-way ANOVA). **D)** Indicated MINK1 KO and MINK1WT cells were treated with 5FU for 48h, after which cell death was determined by annexin V/7AAD assay using flow cytometer. Bar diagrams indicate the percentage of cell death (early and late apoptotic) with respective treated groups (Mean ±SEM, n=3, Two-way ANOVA). **E)** Indicated MINK1 KO and MINK1WT cells were treated with 5 μM of 5FU for 48h, after which immunostaining was performed for γ-H2AX as described in materials ad methods. **F)** Indicated MINK1 KO and MINK1WT cells were treated with 5FU for 48h and immunoblotting was performed with indicated antibodies. **G)** Patient derived cells (PDC2) were earlier established from tumor of chemo-non-responder patient. PDC2 MINK1WT cells were implanted in right upper flank of athymic male nude mice and PDC2 MINK1KO cells were implanted in left upper flank, after which they were treated with 5FU at indicated concentration. At the end of the experiment mice were euthanized, tumors were isolated and photographed (n=5). **H)** Tumor growth was measured in indicated time points using digital slide caliper and plotted as a graph (mean ± SEM, n = 5). Two-way ANOVA. **I)** Bar diagram indicates the tumor weight measured at the end of the experiment (mean ± SEM, n = 5). Two-way ANOVA. **J)** After completion of treatment, tumors were isolated and paraffin-embedded sections were prepared as described in materials and methods to perform immunohistochemistry with indicated antibodies. Scale bars: 50 μm.

Figure 3: Ectopic overexpression of MINK1 rescued the drug resistant phenotype in MINK1KD drug resistant OSCC: A) Using a lentiviral approach, 5FU resistant OSCC lines and PDC2 were stably transfected with ShRNA which targets 3'UTR of MINK1 mRNA (MINK1 UTRKD). For ectopic overexpression, pLenti CMV/TO Puro DEST MINK1 and control vector were transiently transfected to indicated MINK1 UTRKD cells and immunoblotting (n=3) was performed with indicated antibodies. **B)** MINK1 was ectopically overexpressed in 5FUR cells stably expressing MINK1ShRNA targeting UTR and treated with 5FU at indicated concentration for 48 h, after which cell viability was determined by MTT assay (n=3), 2-way ANOVA. **C)** Cells were treated as indicated in B panel and cell death (early and late apoptotic) was determined by annexin V/7AAD assay using flow cytometer. Bar diagrams indicate the percentage of cell death with respective treated groups (Mean ±SEM, n=3), 2-way ANOVA. **D)** MINK1 was overexpressed in 5FUR cells stably expressing MINK1ShRNA targeting UTR and treated with 5FU for 48h, after which immunostaining was performed for γ-H2AX as described in materials and methods. **E)** MINK1 was overexpressed in chemoresistant cells stably expressing MINK1ShRNA targeting 3' UTR, followed by 5FU treatment for 48 hours, and immunoblotting (n = 3) was performed with indicated antibodies. **F)** 5FU sensitive OSCC lines were transfected with pLenti CMV/TO Puro DEST MINK1 followed by treatment with 5FU at indicated concentration for 48h, after which cell viability was determined by MTT assay (n=3), 2-way ANOVA.

Figure 4: MINK1 regulates the expression of p53 in 5FU resistant OSCC lines through AKT/MDM2

A) High-throughput phosphorylation profiling with 1,318 site-specific antibodies from over 30 signaling pathways was performed in the lysates of MINK1KO and MINK1WT clones of H357 5FUR cells as described in methods. The top 20 upregulated phosphoproteins (MINK1

KO/MINK1WT) is represented in left panel, whereas top 20 downregulated phosphorylated proteins is represented in right panel. The upregulated targets considered in the study is marked in green red box, whereas downregulated targets in green box. **B)** Lysates were collected from indicated cells and immunoblotting was performed with indicated antibodies. **C)** pDESTCMV/TO MINK1 (ectopic overexpression of MINK1) was transiently transfected in 5FUR lines stably expressing MINK1 ShRNA (targeting 3'UTR) and immunoblotting was performed with indicated antibodies. **D)** Lysates were collected from indicated cells and immunoblotting was performed with indicated antibodies. **E)** MINK1 was ectopically overexpressed in 5FUR lines stably expressing MINK1 ShRNA (targeting 3'UTR) and immunoblotting was performed with indicated antibodies. **F)** pLNCX myr HA Akt1 (ectopic overexpression of myr AKT) was transiently transfected in indicated MINK1KO cells and immunoblotting was performed with indicated antibodies. **G)** MINK1 was ectopically overexpressed in 5FUR lines stably expressing MINK1ShRNA (UTRKD) as described in panel C and treated with AKT inhibitor (Akti-1/2) for 24h and immunoblotting was performed with indicated antibodies. **H)** Lysates were collected from indicated cells and immunoblotting was performed with indicated antibodies.

Figure 5: Evaluation of Lestaurtinib as a MINK1 inhibitor to restore 5FU sensitivity in drug resistant OSCC: A) *In vitro* MINK1 kinase assay was performed using three compounds potentially binding to MINK1 (based on IUPHAR database). All compounds (10 µM) were incubated with recombinant human MINK1 along with substrate MBP and ATP and further subjected to ADP-Glo™ Kinase Assay as described in materials and methods section. **B)** Determination of EC50 value for kinase activity of top two MINK1 inhibitors selected from panel (A). **C-D)** Selection of highest dose of Lestaurtinib and Pexmetinib that does not affect cell viability when treated alone (viability > 80%) in 5FU resistant OSCC lines (n=3), 2-way ANOVA. **E)** 5FU resistant cells were treated with indicated dose of MINK1 inhibitor (50 nM Lestaurtinib, 500 nM Pexmetinb) in combination with increasing concentrations of 5FU for 48 h, after which cell viability was determined by MTT assay (n=3), 2-way ANOVA. **F)** 5FU resistant OSCC lines and PDC2 cells were treated indicated dose of MINK1 inhibitor (50 nM Lestaurtinib, 500 nM Pexmetinb) in combination with increasing concentrations of 5FU for 48 h, after which cell death (early and late apoptotic) was determined by annexin V/7AAD assay using flow cytometer. Bar diagrams indicate the percentage of cell death with respective treated groups (Mean ±SEM, n=3). Two-way ANOVA. **G)** Indicated 5FU resistant OSCC lines and PDC2 cells were treated with 5 µM of 5FU and/or 50nM of Lestaurtinib for 48h, after which immunostaining was performed for γ-H2AX as described in materials ad methods. **H)** Indicated 5FU resistant OSCC lines and PDC2 cells were treated with 5FU and/or Lestaurtinib for 48h, after which immunoblotting was performed with indicated antibodies. **I)** Effect on 5FU IC50 upon Lestaurtinib treatment in cells with or without MINK1 knockout in indicated 5FU resistant OSCC lines and PDC2 cells (n=3), $*P < 0.05$ by 2-way ANOVA.

Figure 6: Lestaurtinib and 5FU synergistically reduced tumor burden *in vivo* in drug resistant OSCC: A) Patient-derived cells (PDC2) were earlier established from tumor of chemotherapy (TPF) non-responder patient. PDC2 were implanted in the right upper flank of athymic male nude mice, after which they were treated with 5FU and/or Lestaurtinib at indicated concentrations. At the end of the experiment mice were euthanized, and tumors were isolated and photographed (n = 5). **B)** Bar diagram indicates the tumor weight measured at the end of the experiment (mean ± SEM, n = 5). Two-way ANOVA. **C)** Tumor growth was measured at the

indicated time points using digital slide caliper and plotted as a graph (mean ± SEM, n = 5). Two-way ANOVA. **D)** After completion of treatment, tumors were isolated, and paraffin-embedded sections were prepared as described in Methods to perform IHC with indicated antibodies. Scale bars: 50 μm. **E)** Schematic presentation of the mechanism by which MINK1 regulates p53 expression through AKT/MDM2 axis**.**

Figure 01

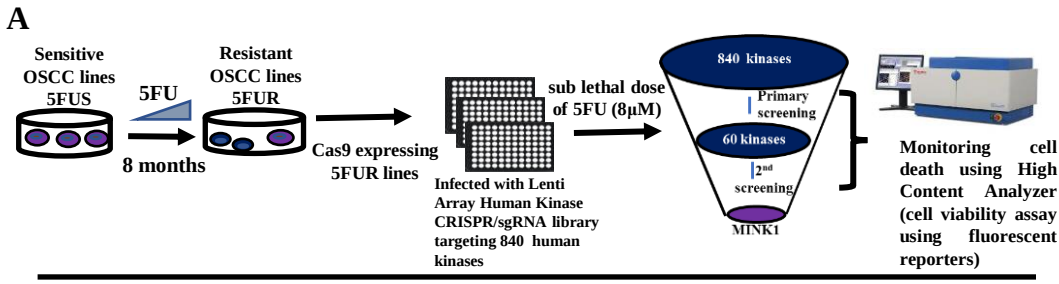

Strategy for CRISPR based kinome knock out screening in 5FU resistant OSCC lines

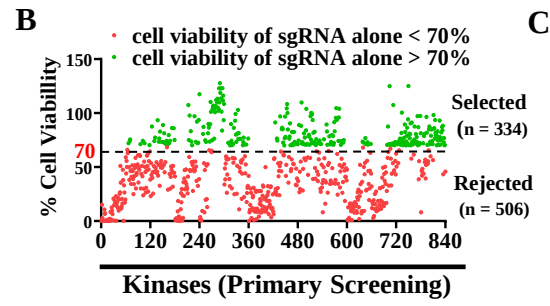

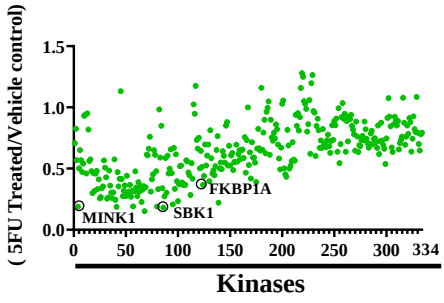

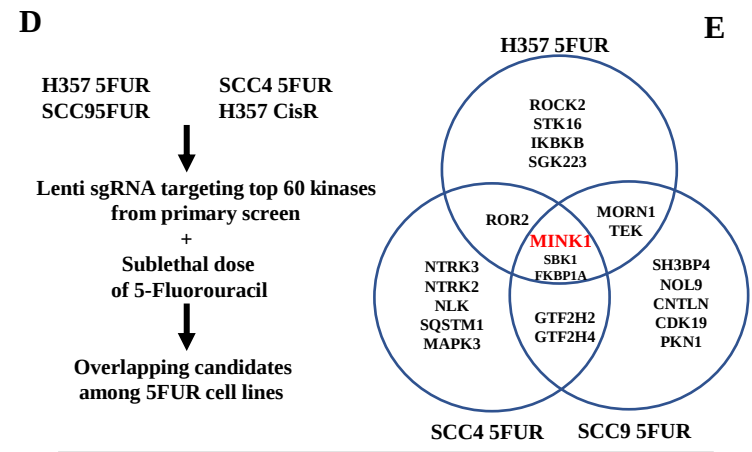

Secondary kinome screening in 5FU resistant OSCC

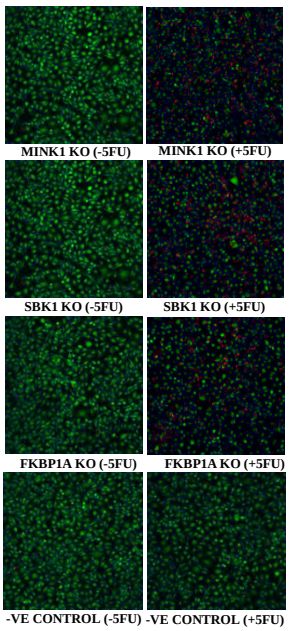

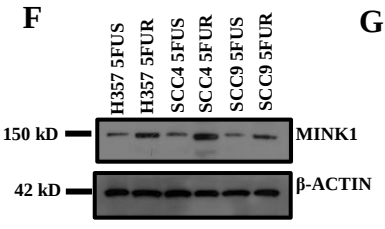

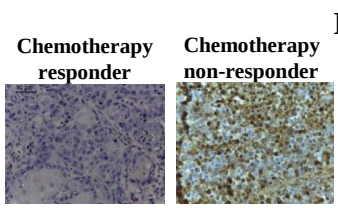

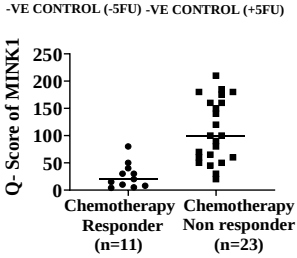

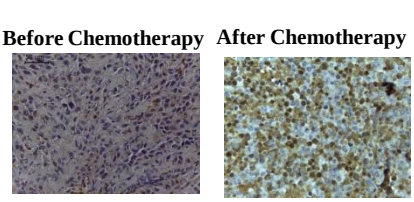

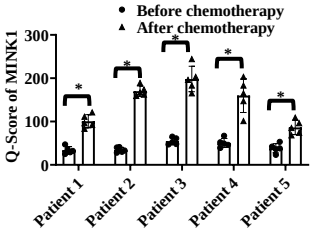

Figure 02

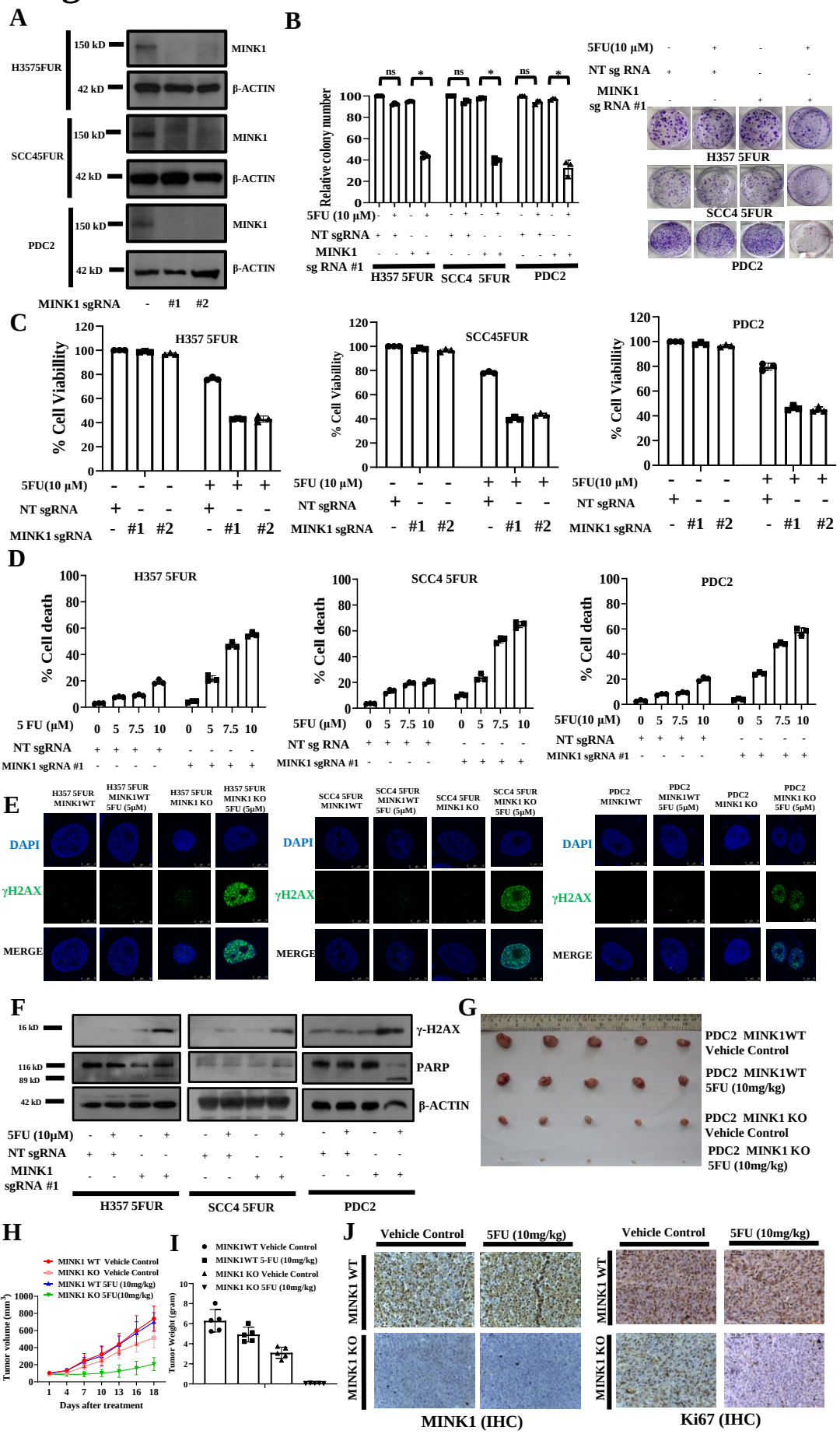
A
H3575FUR
SCC45FUR
PDC2
150 kD
42 kD
MINK1
β-ACTIN
MINK1 sgRNA - #1 #2
B
Relative colony number
ns
*
5FU (10 μM)
NT sgRNA
MINK1 sg RNA #1
H357 5FUR
SCC4 5FUR
PDC2
5FU(10 μM)
NT sg RNA
MINK1 sg RNA #1
C
% Cell Viability
H357 5FUR
SCC45FUR
PDC2
5FU(10 μM)
NT sgRNA
MINK1 sgRNA
D
% Cell death
H357 5FUR
SCC4 5FUR
PDC2
5 FU (μM)
5FU (μM)
5FU(10 μM)
NT sgRNA
NT sg RNA
MINK1 sgRNA #1
E
H357 5FUR MINK1WT
H357 5FUR MINK1WT 5FU (5μM)
H357 5FUR MINK1 KO
H357 5FUR MINK1 KO 5FU (5μM)
SCC4 5FUR MINK1WT
SCC4 5FUR MINK1WT 5FU (5μM)
SCC4 5FUR MINK1 KO
SCC4 5FUR MINK1 KO 5FU (5μM)
PDC2 MINK1WT
PDC2 MINK1WT 5FU (5μM)
PDC2 MINK1 KO
PDC2 MINK1 KO 5FU (5μM)
DAPI
γH2AX
MERGE
F
16 kD
116 kD
89 kD
42 kD
γ-H2AX
PARP
β-ACTIN
5FU (10μM)
NT sgRNA
MINK1 sgRNA #1
H357 5FUR
SCC4 5FUR
PDC2
G
PDC2 MINK1WT Vehicle Control
PDC2 MINK1WT 5FU (10mg/kg)
PDC2 MINK1 KO Vehicle Control
PDC2 MINK1 KO 5FU (10mg/kg)
H
MINK1 WT Vehicle Control
MINK1 KO Vehicle Control
MINK1 WT 5FU (10mg/kg)
MINK1 KO 5FU(10mg/kg)
Tumor volume (mm³)
Days after treatment
I
MINK1WT Vehicle Control
MINK1WT 5-FU (10mg/kg)
MINK1 KO Vehicle Control
MINK1 KO 5FU (10mg/kg)
Tumor Weight (gram)
J
Vehicle Control
5FU (10mg/kg)
MINK1 WT
MINK1 KO
MINK1 (IHC)
Ki67 (IHC)

Figure 03

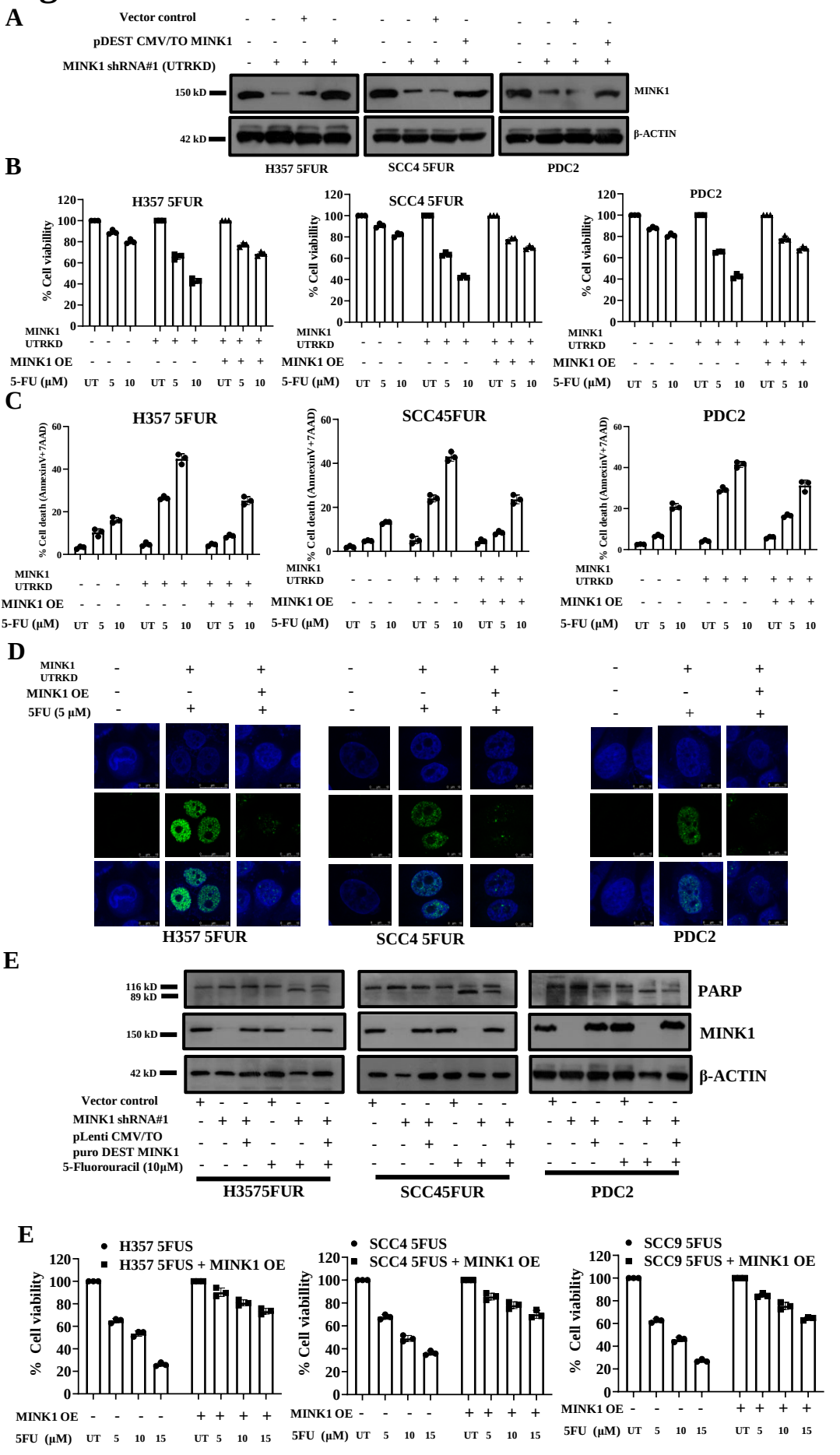
A
Vector control
pDEST CMV/TO MINK1
MINK1 shRNA#1 (UTRKD)
150 kD
42 kD
MINK1
β-ACTIN
H357 5FUR
SCC4 5FUR
PDC2
B
H357 5FUR
SCC4 5FUR
PDC2
% Cell viability
MINK1 UTRKD
MINK1 OE
5-FU (μM)
UT 5 10
C
H357 5FUR
SCC45FUR
PDC2
% Cell death (AnnexinV+7AAD)
D
MINK1 UTRKD
MINK1 OE
5FU (5 μM)
H357 5FUR
SCC4 5FUR
PDC2
E
116 kD
89 kD
150 kD
42 kD
PARP
MINK1
β-ACTIN
Vector control
MINK1 shRNA#1
pLenti CMV/TO puro DEST MINK1
5-Fluorouracil (10μM)
H3575FUR
SCC45FUR
PDC2
E
H357 5FUS
H357 5FUS + MINK1 OE
SCC4 5FUS
SCC4 5FUS + MINK1 OE
SCC9 5FUS
SCC9 5FUS + MINK1 OE
% Cell viability
MINK1 OE
5FU (μM)
UT 5 10 15

Figure 04

A

Phosphorylated proteins	Phosphorylation ratio of MINK1 KO/ WT
p53 (Phospho-Ser33)	2.387529
ALK (Phospho-Tyr1507)	2.187586
GSK3 beta (Phospho-Ser9)	2.172644
Gab2 (Phospho-Tyr643)	2.016842
AKT1S1 (Phospho-Thr246)	2.008168
p53 (Phospho-Ser15)	1.920548
c-Jun (Phospho-Ser63)	1.897019
Catenin beta (Phospho-Tyr654)	1.799196
Keratin 8 (Phospho-Ser432)	1.757952
IL-13R/CD213a1 (Phospho-Tyr405)	1.646146
Dok-2 (Phospho-Tyr299)	1.604889
VEGFR2 (Phospho-Tyr1175)	1.60054
GSK3 alpha (Phospho-Ser21)	1.588892
Androgen Receptor (Phospho-Ser213)	1.566496
Tau (Phospho-Thr181)	1.565912
IGF2R (Phospho-Ser2489)	1.56576
eIF2A (Phospho-Ser51)	1.559497
CDK5 (Phospho-Tyr15)	1.547983
14-3-3 zeta (Phospho-Ser58)	1.522109
4E-BP1 (Phospho-Thr45)	1.505419

Phosphorylated proteins	Phosphorylation ratio of MINK1 KO/ WT
HDAC1 (Phospho-Ser421)	0.32937
AKT1 (Phospho-Ser473)	0.351857
LYN (Phospho-Tyr507)	0.356728
Abl1 (Phospho-Tyr204)	0.403395
HSL (Phospho-Ser554)	0.409255
ATP1A1/Na+K+ ATPase1 (Phospho-Ser23)	0.454414
EEF2 (Phospho-Thr56)	0.47177
TYK2 (Phospho-Tyr1054)	0.506242
JAK2 (Phospho-Tyr1007)	0.532182
Chk2 (Phospho-Ser516)	0.538779
FLT3 (Phospho-Tyr599)	0.558251
EGFR (Phospho-Tyr869)	0.560672
GluR1 (Phospho-Ser849)	0.581223
AurB (Phospho-Thr232)	0.590025
AKT2 (Phospho-Ser474)	0.594925
Integrin beta-1 (Phospho-Thr788)	0.595157
DYN1 (Phospho-Ser774)	0.596312
MDM2 (Phospho-Ser166)	0.61482
IL-2RA/CD25 (Phospho-Ser268)	0.627742
Caspase 9 (Phospho-Tyr153)	0.630743

B

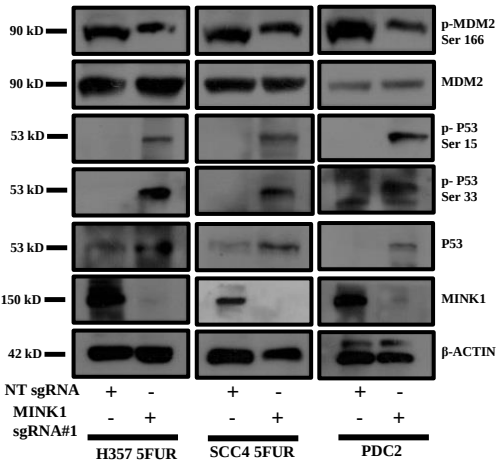

C

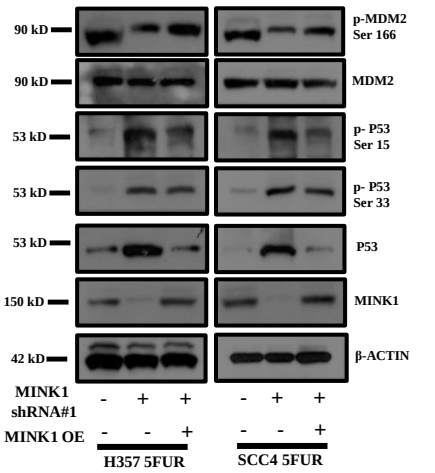

D

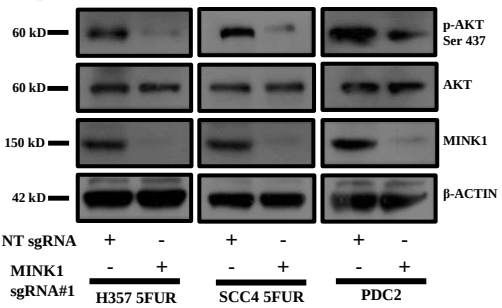

E

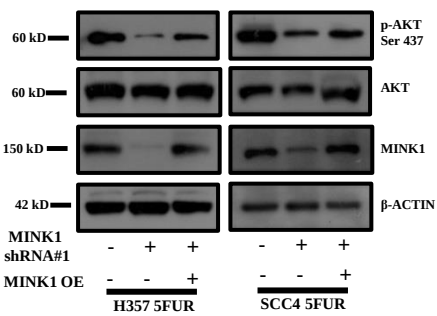

F

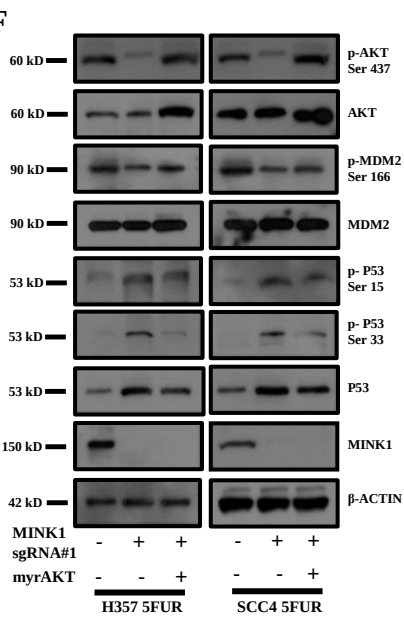

G

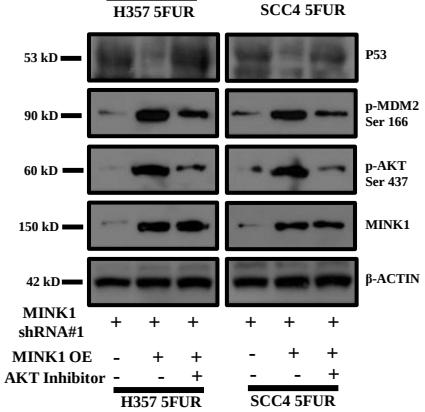

H

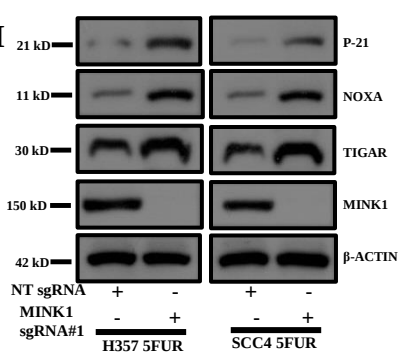

Figure 05

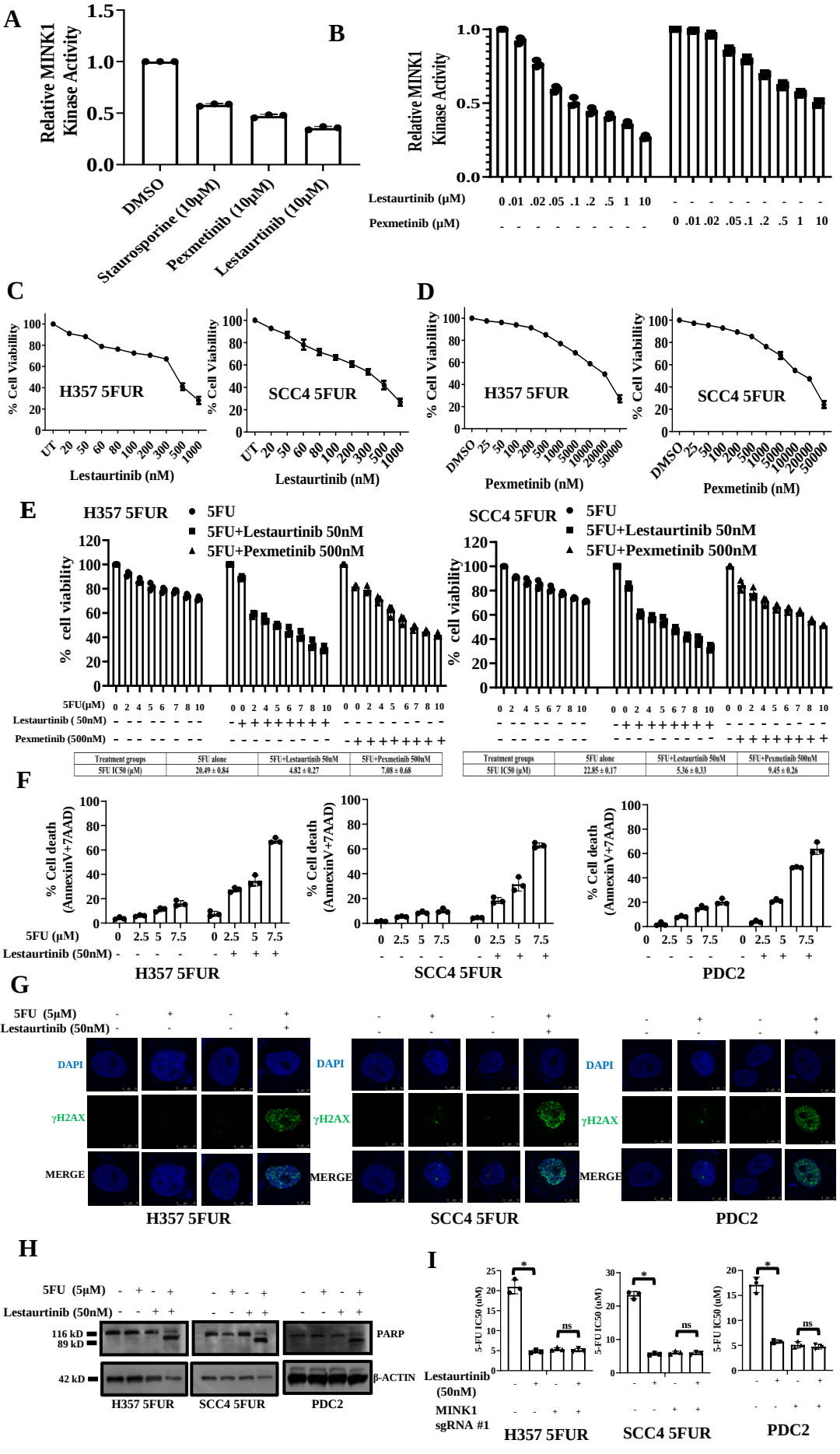
A
Relative MINK1 Kinase Activity
1.5
1.0
0.5
0.0
DMSO
Staurosporine (10μM)
Pexmetinib (10μM)
Lestaurtinib (10μM)
B
Relative MINK1 Kinase Activity
1.0
0.5
0.0
Lestaurtinib (μM) 0 .01 .02 .05 .1 .2 .5 1 10
Pexmetinib (μM) 0 .01 .02 .05 .1 .2 .5 1 10
C
% Cell Viability
H357 5FUR
UT 20 50 60 80 100 200 300 500 1000
Lestaurtinib (nM)
% Cell Viability
SCC4 5FUR
UT 20 50 60 80 100 200 300 500 1000
Lestaurtinib (nM)
D
% Cell Viability
H357 5FUR
DMSO 25 50 100 200 500 1000 5000 10000 20000 50000
Pexmetinib (nM)
% Cell Viability
SCC4 5FUR
DMSO 25 50 100 200 500 1000 5000 10000 20000 50000
Pexmetinib (nM)
E
H357 5FUR
5FU
5FU+Lestaurtinib 50nM
5FU+Pexmetinib 500nM
% cell viability
5FU(μM) 0 2 4 5 6 7 8 10 0 0 2 4 5 6 7 8 10 0 0 2 4 5 6 7 8 10
Lestaurtinib (50nM) - - - - - - - - + + + + + + + - - - - - - - -
Pexmetinib (500nM) - - - - - - - - - - - - - - - - + + + + + + + +
Treatment groups | 5FU alone | 5FU+Lestaurtinib 50nM | 5FU+Pexmetinib 500nM
5FU IC50 (μM) | 20.49 ± 0.84 | 4.82 ± 0.27 | 7.08 ± 0.68
SCC4 5FUR
5FU
5FU+Lestaurtinib 50nM
5FU+Pexmetinib 500nM
% cell viability
0 2 4 5 6 7 8 10 0 0 2 4 5 6 7 8 10 0 0 2 4 5 6 7 8 10
- - - - - - - - + + + + + + + - - - - - - - -
- - - - - - - - - - - - - - - - + + + + + + + +
Treatment groups | 5FU alone | 5FU+Lestaurtinib 50nM | 5FU+Pexmetinib 500nM
5FU IC50 (μM) | 22.85 ± 0.17 | 5.36 ± 0.33 | 9.45 ± 0.26
F
% Cell death (AnnexinV+7AAD)
5FU (μM) 0 2.5 5 7.5 0 2.5 5 7.5
Lestaurtinib (50nM) - - - - - + + +
H357 5FUR
% Cell death (AnnexinV+7AAD)
0 2.5 5 7.5 0 2.5 5 7.5
- - - - - + + +
SCC4 5FUR
% Cell death (AnnexinV+7AAD)
0 2.5 5 7.5 0 2.5 5 7.5
- - - - - + + +
PDC2
G
5FU (5μM) - + - + - + - + - + - +
Lestaurtinib (50nM) - - - + - - - + - - - +
DAPI
γH2AX
MERGE
H357 5FUR
SCC4 5FUR
PDC2
H
5FU (5μM) - + - + - + - + - + - +
Lestaurtinib (50nM) - - + + - - + + - - + +
116 kD
89 kD
PARP
42 kD
β-ACTIN
H357 5FUR
SCC4 5FUR
PDC2
I
5-FU IC50 (nM)
*
ns
Lestaurtinib (50nM)
MINK1 sgRNA #1
H357 5FUR
SCC4 5FUR
PDC2

Figure 06

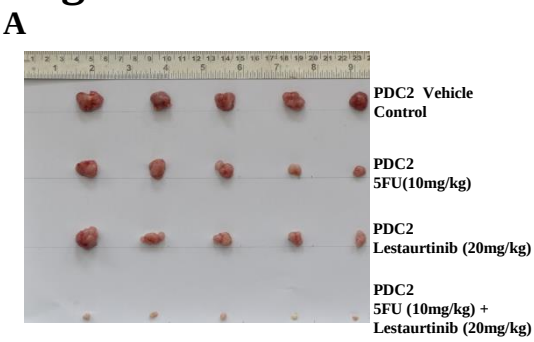

5FU Resistant OSCC cells

Table S1a

chemotherapy-responder patient details

Sl No	Tumor samples	Age/Sex	Site of disease	Clinical stage	Chemotherapy (NACT)	Cycle
1	**Patient#1**	42/M	Tongue Rt lateral border	T4aN1M0	Docetaxel + Cisplatin+ 5FU	2
2	**Patient#2**	67/M	Tongue Lt lateral border	T4aN1Mx	Docetaxel + Cisplatin+ 5FU	3
3	**Patient#3**	50/M	Rt- Buccal mucosa	T4aN2bM0	Docetaxel + Cisplatin+ 5FU	3
4	**Patient#4**	75/M	Oral cavity	T3N2bM0	Doceaqualip + Carboplatin	3
5	**Patient#5**	46/M	Tongue	T3N1M0	Docetaxel + Cisplatin+ 5FU	3
6	**Patient#6**	35/M	Tongue	T4aN2eM0	Docetaxel + Cisplatin+ 5FU	3
7	**Patient#7**	38/M	Right Buccal Mucosa	T4bN2bM0	Docetaxel + Cisplatin+ 5FU	3
8	**Patient#8**	34/M	Left Buccal Mucosa	T4aN2bMx	Docetaxel + Cisplatin+ 5FU	3
9	**Patient#9**	40/M	Tongue	T2N2cM0	Docetaxel + Cisplatin+ 5FU	3
10	**Patient#10**	45/M	Tongue	T2N1M0	Docetaxel + Cisplatin+ 5FU	3
11	**Patient#11**	51/M	Tongue Lt. lateral border	T4aN2cM0	Docetaxel + Cisplatin+ 5FU	3

Chemotherapy Doses: **Cisplatin**: 100mg. **Docetaxel**: 100mg, **5FU**:1000mg, **Doceaqualip**: 80mg, **Carboplatin:** AUC 4 (area under the ROC curve)

Table S1b

Chemotherapy-non-responders patient Details

Sl No	Tumor samples	Age /Sex	Site of disease	Clinical stage	Chemotherapy (NACT)	Cycle
1	Patient# 1	76/M	Tongue Rt lateral border	T4N0M0	Paclitaxel + Cisplatin	3
2	Patient#2 (PDC#2)	51/M	Rt- Buccal mucosa	T2N2bM0	Docetaxel + Cisplatin+ 5FU	2
3	Patient# 3	60/M	Tongue Rt lateral border	T3N1M0	Paclitaxel + Cisplatin +5FU	3
4	Patient#4	33/M	Rt- Lower Alveolar mucosa	T3N1Mx	Docetaxel + Cisplatin	3
5	Patient#5	60/F	Tongue Lt lateral border	T4N0M0	Docetaxel + Cisplatin+ 5FU	3
6	Patient#6	59/M	Tongue Rt lateral border	T4aN1M0	Docetaxel + Cisplatin+ 5FU	3
7	Patient#7	46/M	Tongue	T4N3M0	Docetaxel + Cisplatin+ 5FU	3
8	Patient#8	55/F	Rt- Buccal Mucosa	T4aN2M0	Docetaxel + Cisplatin+ 5FU	2
9	Patient#9	37/M	Tongue	T4N3M0	Docetaxel + Cisplatin+ 5FU	2
10	Patient#10	27/M	Lt-Buccal Mucosa	T4N2M0	Docetaxel + Cisplatin+ 5FU	2
11	Patient#11	46/F	Rt- oral cavity	T4N1M0	Docetaxel + Cisplatin+ 5FU	3
12	Patient#12	42/M	Rt- Buccal Mucosa	TxN3bM0	Paclitaxel + Cisplatin+ 5FU	2
13	Patient#13	30/M	Tongue Rt lateral border	T2N0Mx	Paclitaxel + Cisplatin+ 5FU	3
14	Patient#14	52/M	Rt- Buccal Mucosa	T4N2M0	Docetaxel + Cisplatin+ 5FU	3
15	Patient#15	32/M	Tongue	T3N1M0	Docetaxel + Cisplatin+ 5FU	3
16	Patient#16	35/M	Tongue	T4aN2aM0	Docetaxel + Cisplatin+ 5FU	3
17	Patient#17	36/M	Left Buccal Mucosa	T4aN2aM0	Docetaxel + Cisplatin+ 5FU	3
18	Patient #18	38/M		T4bN2bMO	Docetaxel + Cisplatin+ 5FU	2
19	Patient # 19	55/M	Tongue, Left lateral border,		Docetaxel + Cisplatin+ 5FU	3
20	Patient # 20	35/M	Tongue	T4aN2eM0+	Docetaxel + Cisplatin+ 5FU	3
21	Patient # 21	36/M	Left Buccal Mucosa	cT4aN2aM0	Docetaxel + Cisplatin+ 5FU	3
22	Patient # 22	39/M	Right mandible	cT4bN0Mx	Docetaxel + Cisplatin+ 5FU	3
23	Patient # 23	55/M	Tongue, Left lateral border,	cT4aN2cM0	Docetaxel + Cisplatin+ 5FU	3

chemotherapy taken, but after 1-2 cycles became non responded.

Chemotherapy Doses: **Cisplatin**: 100mg. **Paclitaxe**l: 260 mg, **Docetaxel**: 100mg, **5FU**:1000mg **Lt-Left, Rt-Right**

PDC2: patient derived cells isolated from indicated OSCC patients.

Table S2

Oligos for SgRNA and ShRNA

Sg and Sh RNA primers	Oligo sequence
MINK1 sg RNA F (SgRNA#1)	CACCCGCAACATCGCCACCTACTA
MINK1 sg RNA R (SgRNA#1)	AAACTAGTAGGTGGCGATGTTGCG
MINK1 sg RNA F (SgRNA#2)	CACCGTGGTCGGCAATGGAACCTA
MINK1 sg RNA R (SgRNA#2)	AAACTAGGTTCCATTGCCGACCAC
MINK1 3' UTR sh RNA F (ShRNA#1)	CCGGAATGTAGTGGCCTTGGATATCCTCGAGGATATCCAAGGCCACTACATTTTTTTG
MINK1 3' UTR sh RNA R (ShRNA#1)	AATTCAAAAAAATGTAGTGGCCTTGGATATCCTCGAGGATATCCAAGGCCACTACATT

Oligos for qRT-PCR

qRT PCR Primers	Primer sequence
18S qRT F	GTAACCCGTTGAACCCCATT
18S qRT R	CCATCCAATCGGTAGTAGCG
GAPDH qRT F	TCGGAGTCAACGGATTTGGT
GAPDH qRT R	TTGCCATGGGTGGAATCATA
OCT4 qRT F	CGACCATCTGCCGCTTTGAG
OCT4 qRT R	CCCCCTGTCCCCCATTCCTA
SOX2 qRT F	CACCTACAGCATGTCCTACTC
SOX2 qRT R	CATGCTGTTTCTTACTCTCCTC
Nanog qRT F	CAACTGGCCGAAGAATAGCA
Nanog qRT R	GCAGGAGAATTTGGCTGGAA
ABCC1 qRT F	AGTGGAACCCCTCTCTGTTTAAG
ABCC1 qRT R	CCTGATACGTCTTGGTCTTCATC
ABCC2 qRT F	AATCAGAGTCAAAGCCAAGATGCC
ABCC2 qRT R	TAGCTTCAGTAGGAATGATTTCAGGAGCAC
ABCC3 qRT F	TCCTTTGCCAACTTTCTCTGCAACTAT
ABCC3 qRT R	CTGGATCATTGTCTGTCAGATCCGT
ABCC4 qRT F	TGATGAGCCGTATGTTTTGC
ABCC4 qRT R	CTTCGGAACGGACTTGACAT
ABCC5 qRT F	AGAGGTGACCTTTGAGAACGCA
ABCC5 qRT R	CTCCAGATAACTCCACCAGACGG
ABCG2 qRT F	CCGCGACAGTTTCCAATGACCT
ABCG2 qRT R	GCCGAAGAGCTGCTGAGAACTGTA
MDR1 qRT F	AGGAAGCCAATGCCTATGACTTTA
MDR1 qRT R	CAACTGGGCCCCTCTCTCTC

Oligos to detect genomic cleavage detection assays

HPRT1 GCD F	TACACGTGTGAACCAACCCG
HPRT1 GCD R	GTAAGGCCCTCCTCTTTTATTT

Supplementary Figure 01

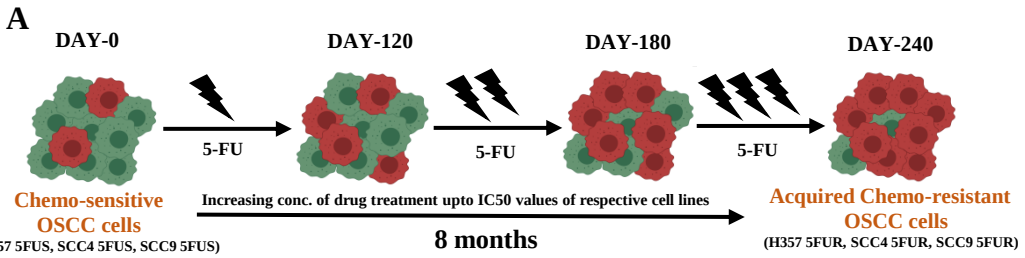

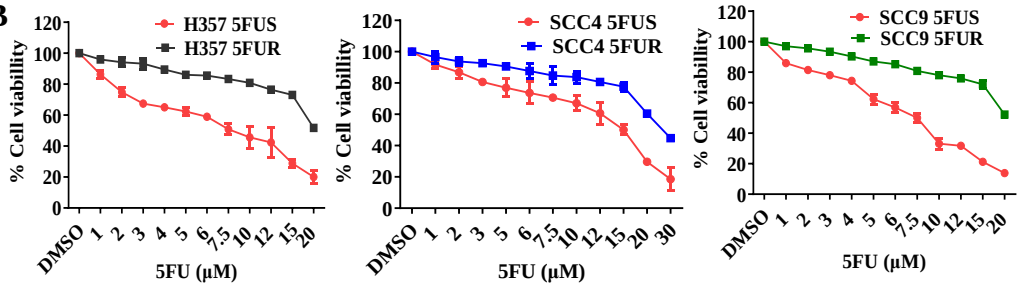

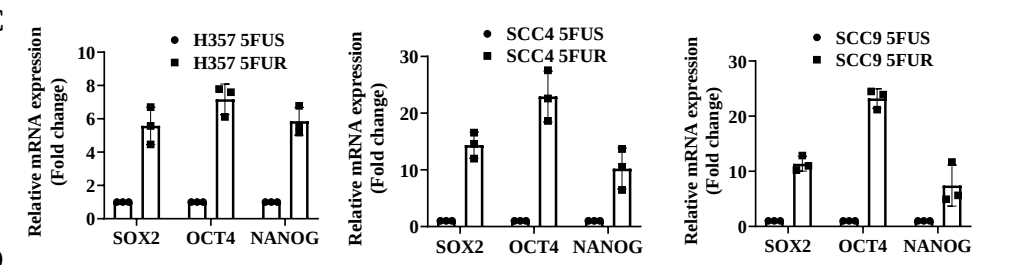

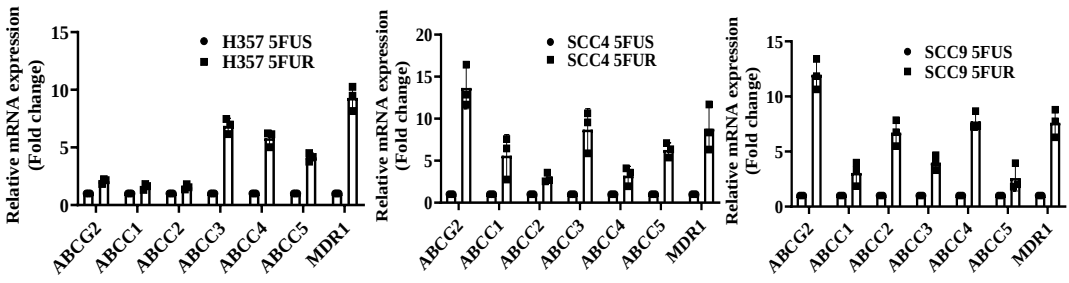

Supplementary Figure 02

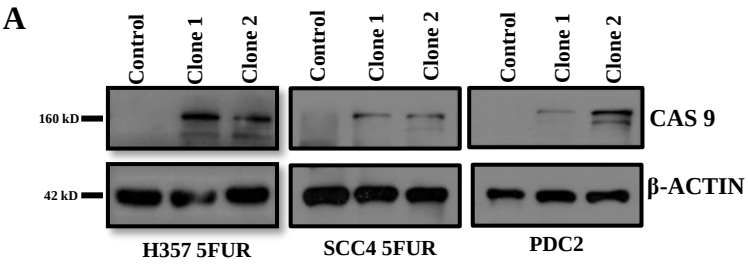

Supplementary Figure 03

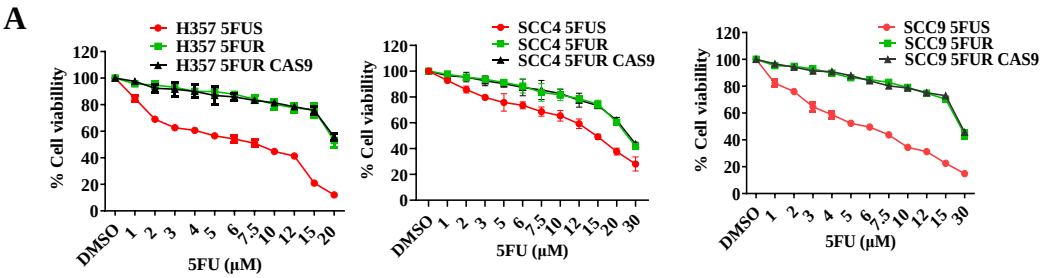

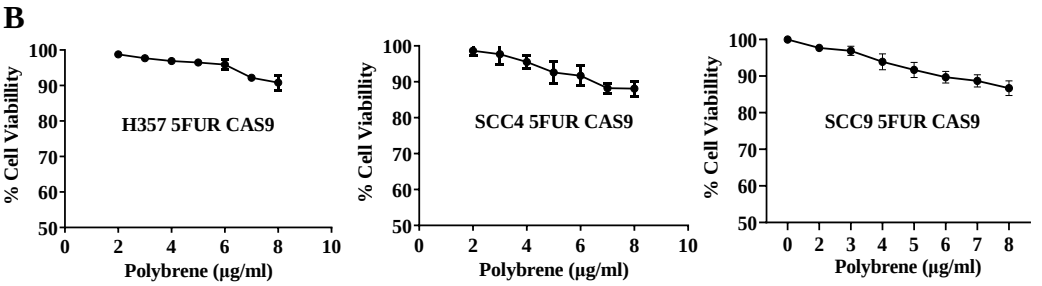

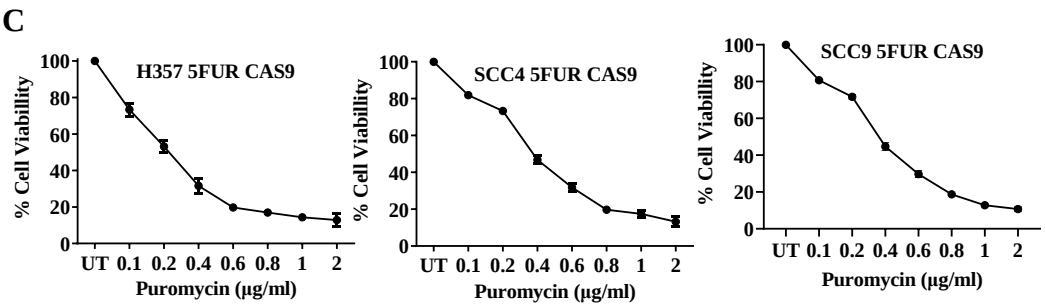

Supplementary Figure 04

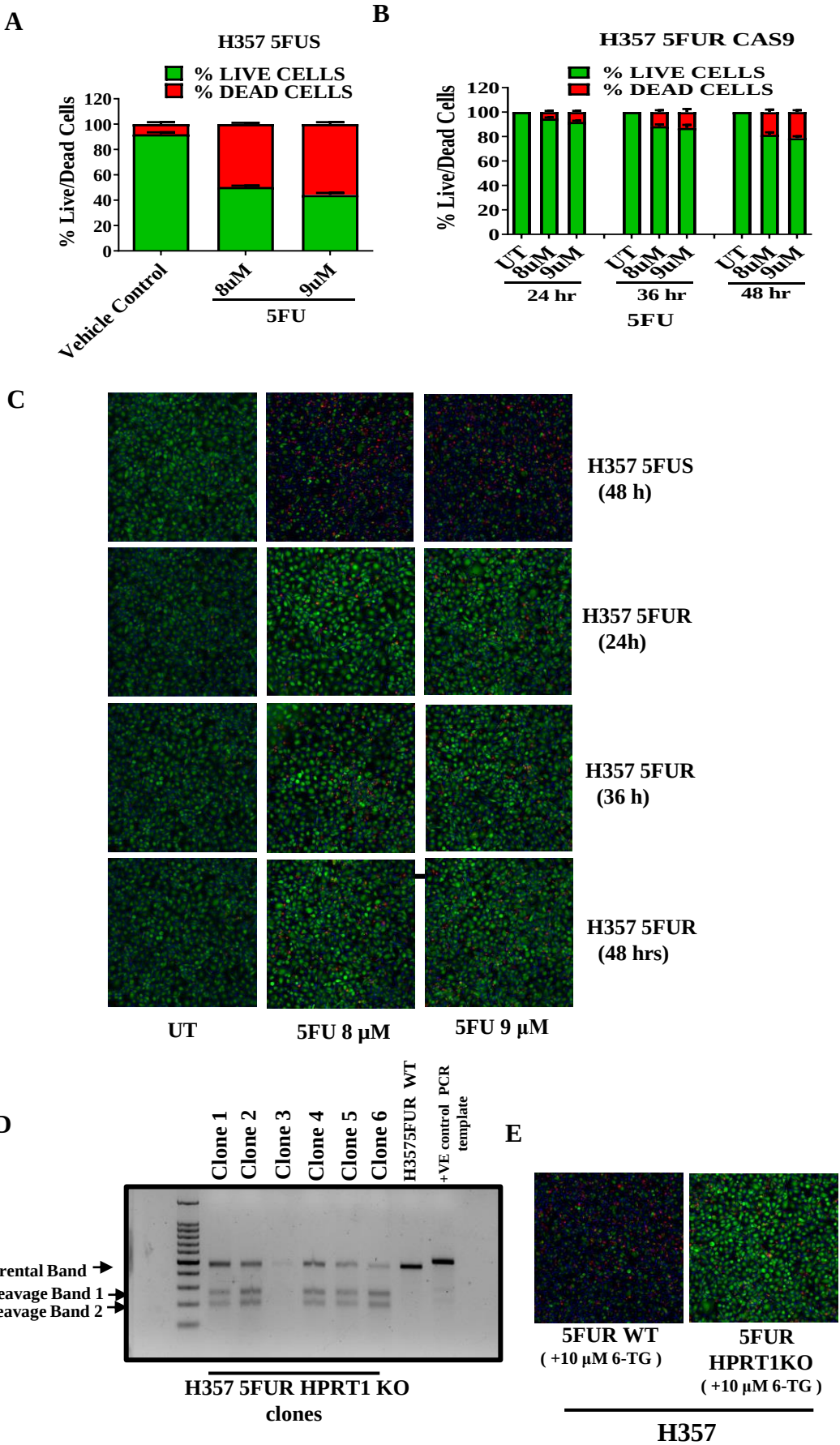

Supplementary Figure 05

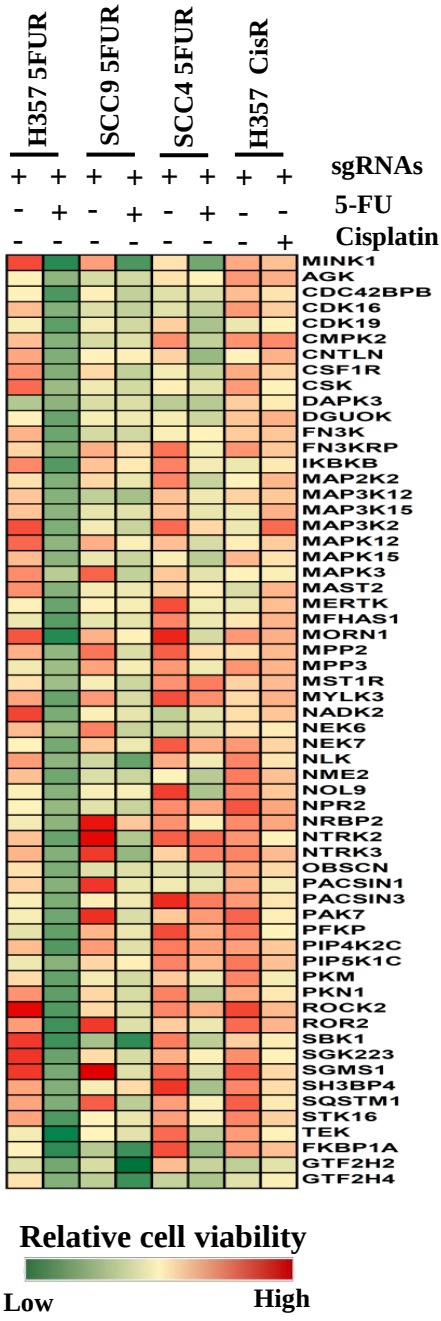

Supplementary Figure 06

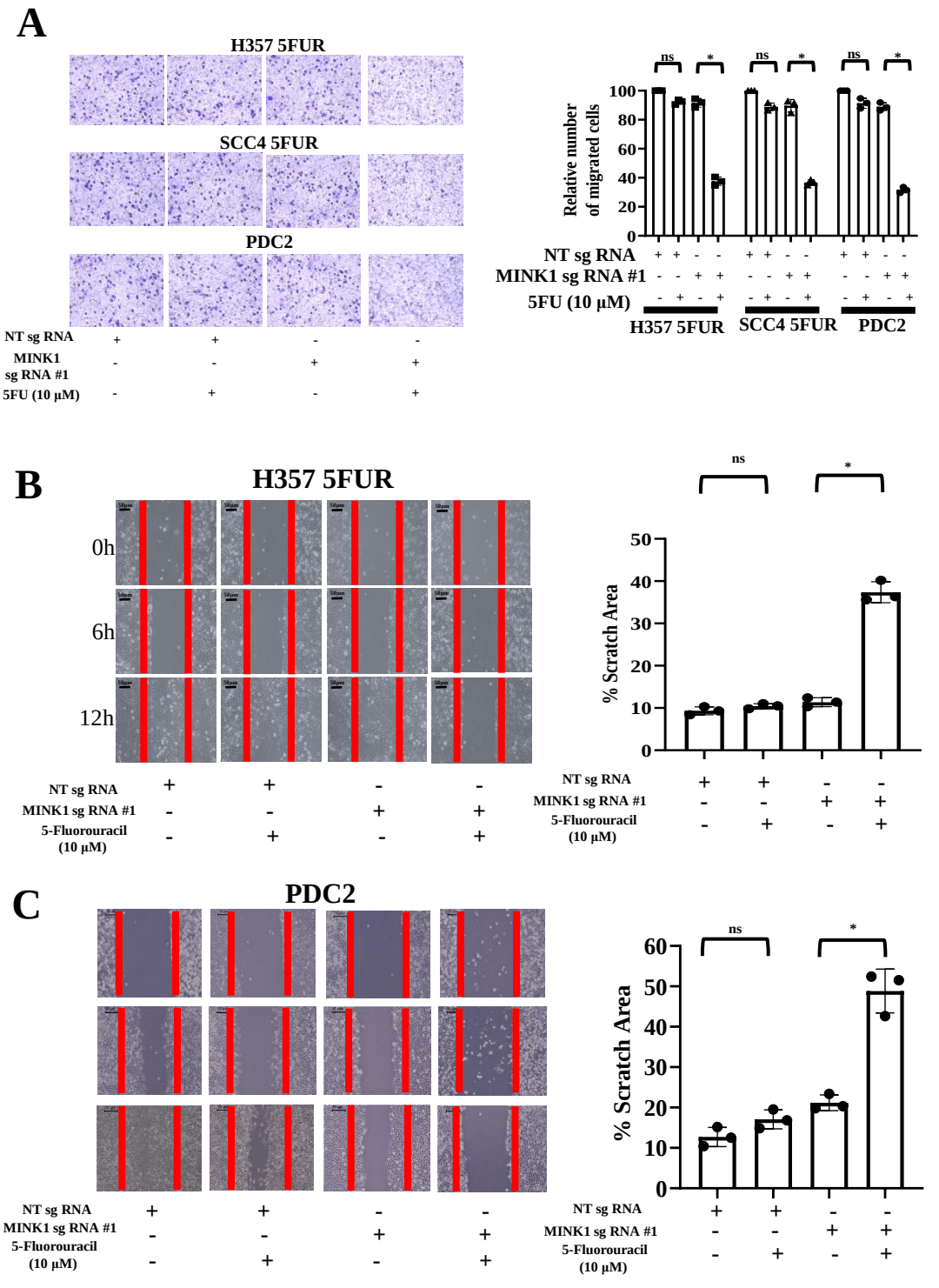

Supplementary Figure 07

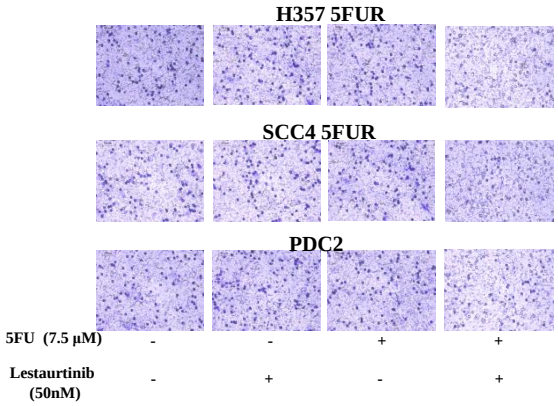

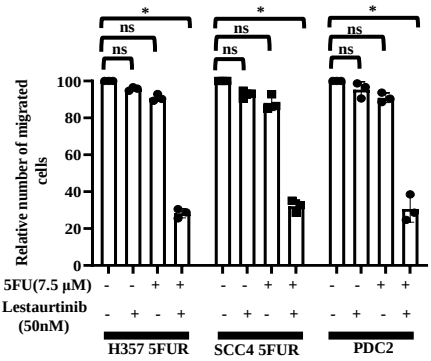

Supplementary Figure 08

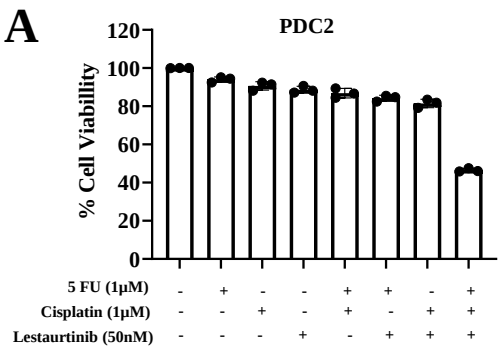

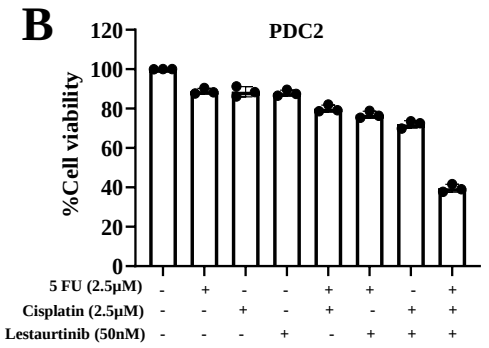

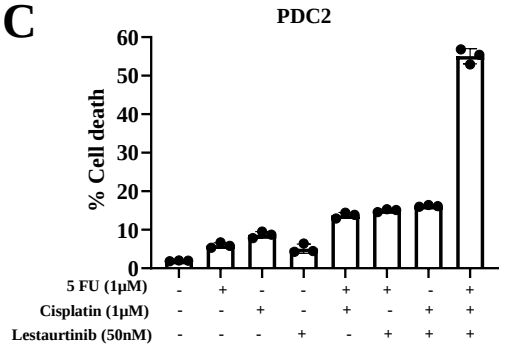

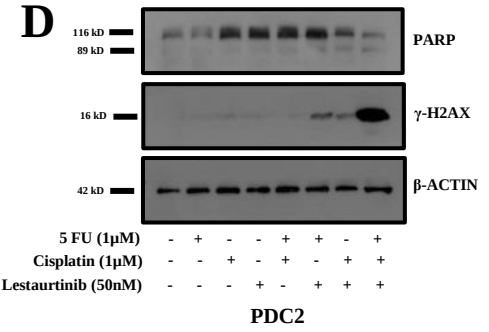

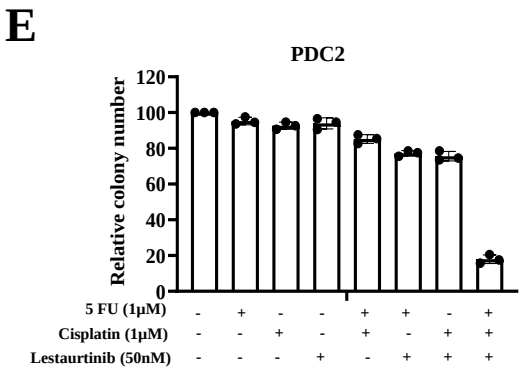

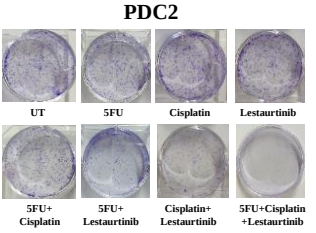

Figure S1: Characterization of sensitive and 5FU resistant OSCC lines: A) Schematic presentation of approach for establishing 5FU resistant OSCC lines **B)** Sensitive and 5FU resistant pattern (5FUS and 5FUR) of H357, SCC4 and SCC9 cells were treated with indicated concentrations of 5FU for 48h and cell viability was determined by MTT assay (n=3, *: $P < 0.05$). 2-way ANOVA. **C-D)** RNA was isolated from Sensitive and 5FU resistant pattern (5FUS and 5FUR) of H357, SCC4 and SCC9 cells and relative mRNA (fold change) expression of indicated genes was analyzed by qRT-PCR (mean ± SEM, n = 3), 2-way ANOVA.

Figure S2: Overexpression of Cas9 in 5FU resistant OSCC lines and PDC: A) Lysates were collected from indicated cells and immunoblotting was performed with indicated antibodies.

Figure S3: Characterization of Cas9 overexpressing OSCC lines regarding 5FU resistance, polybrene tolerance and puromycin sensitivity: A) Indicated sensitive, 5FU resistant, 5FU resistant Cas9 overexpressing cells were treated with indicated concentrations of 5FU for 48h and cell viability was determined by MTT assay (n=3 and *$P < 0.05$ by 2-way ANOVA). **B)** Indicated 5FU resistant Cas9 overexpressing cells were treated with indicated concentrations of polybrene for 48h and cell viability was determined by MTT assay (n=3 and *$P < 0.05$ by 2-way ANOVA). **C)** Indicated 5FU resistant Cas9 overexpressing cells were treated with indicated concentrations of puromycin for 48h and cell viability was determined by MTT assay (n=3 and *$P < 0.05$ by 2-way ANOVA).

Figure S4: Validation of 5FU resistance and optimization of kinome screening conditions using high content analyzer: A-B) 5FU sensitive and resistant patterns of H357 cells were treated with indicated concentrations of 5FU for the indicated time points, after which cell viability was measured in high content analyzer using a live/dead cell imaging kit. **C)** The representative fluorescent images acquired from high content analyzer with indicated treated groups in indicated cells. **D)** Different HPRT1 KO clones in H357 5FUR cells were subjected to genomic cleavage detection assay as described in materials and methods section. **E)** The representative fluorescent images acquired from high content analyzer with indicated treated groups in indicated cells.

Figure S5: Secondary screening identifies MINK1 as a common target among different 5FU resistant OSCC lines: The top 60 candidates resulting from the primary screening were subjected to secondary screening in three different 5FU resistant OSCC lines along with one cisplatin resistant OSCC line. The relative cell viability is presented in the form of heat map.

Figure S6: MINK1 genomic ablation negatively affects tumor cell migration in OSCC: A) Indicated MINK1 WT and KO cells were treated with vehicle control or 5FU (10 μM) for 48h and were subjected to Boyden chamber assay as described in materials and methods section. Left panel: representative photographs of Boyden chamber assay in each group. Right panel: Bar diagrams indicate the relative number of migrated cells (n=3 and *$P < 0.05$ by 2-way ANOVA). Scale bars: 50 μm. **B-C)** Indicated MINK1 WT and KO cells were treated with vehicle control or 5FU (10 μM) for 48h and were subjected to scratch assay as described in materials and methods section. Left panel : representative photographs of scratch assay in each group. Right panel : Bar diagrams indicate the percentage scratch area (n=3 and *$P < 0.05$ by 2-way ANOVA). Scale bars: 50 μm.

Figure S7: Lestaurtinib negatively affects tumor cell migration in OSCC: Indicated 5FU resistant OSCC lines and PDC cells were treated with vehicle control, 5FU (7.5 μM) and/or lestaurtinb (50 nM) for 48h, followed by subjecting to Boyden chamber assay. Left panel: representative photographs of Boyden chamber assay in each group. Right panel: Bar diagrams indicate the relative number of migrated cells (n=3 and $*P < 0.05$ by 2-way ANOVA). Scale bars: 50 μm.

Figure S8: Evaluation of combinatorial anti-tumor effect of low dose of cisplatin, 5FU and lestaurtinb in TPF resistant patient derived cells (PDC2). A-B) PDC2 cells were treated with indicated concentrations of cisplatin, 5FU and lestaurtinib for 48h and cell viability was measured by MTT assay(n=3 and $*P < 0.05$ by 2-way ANOVA). **C)** PDC2 cells were treated with indicated concentrations of cisplatin, 5FU and lestaurtinib for 48h after which cell death was determined by annexin V/7AAD assay using flow cytometer. Bar diagrams indicate the percentage of cell death (early and late apoptotic) with respective treated groups (Mean ±SEM, n=3 by Two-way ANOVA). **D)** PDC2 cells were treated with indicated concentrations of cisplatin, 5FU and lestaurtinib for 48h and immunoblotting was performed with indicated antibodies. **E)** PDC2 cells were treated with indicated concentrations of cisplatin, 5FU, lestaurtinib for 12 days and colony forming assays were performed as described in method section. Left panel: Bar diagram indicate the relative colony number (n=3 and $*P < 0.05$ by 2-way ANOVA). Right panel: representative photographs of colony forming assay in each group.